THE $D(p,\gamma)He^3$ REACTION AT LOW ENERGIES

by

Ernest Andrew Gustav Larson

A THESIS SUBMITTED IN PARTIAL FULFILMENT OF

THE REQUIREMENTS FOR THE DEGREE OF

MASTER OF ARTS

in the Department of

PHYSICS

We accept this thesis as conforming to the standard

required from candidates for the degree of

MASTER OF ARTS

Members of the Department of Physics

THE UNIVERSITY OF BRITISH COLUMBIA

October, 1957

ABSTRACT

A detailed study has been made of the $D(p, \gamma)He^3$ reaction at proton energies of 300 kev, 600 kev, and 1.0 Mev.

In order to measure the absolute cross section for this reaction the efficiency of a 2.5 inch by 3.5 inch sodium iodide crystal scintillation counter was measured by simultaneous alpha particle and gamma ray measurements on the 340 kev resonance of F^{19} $(p, \alpha, \gamma)O^{16}$. The efficiency of the counter for the 6.14 Mev gamma radiation from this resonance has a measured value of 0.612 ± 0.009.

The angular distribution of the gamma radiation from the $D(p, \gamma)He^3$ reaction has been found to have the form $A(\sin^2\theta + b)$ where b equals 0.0795 ± 0.010, 0.032 ± 0.004 and 0.024 ± 0.003 at proton energies of 300 kev, 600 kev and 1.0 Mev respectively.

The absolute cross section of this reaction has been measured at proton energies of 300 kev and 1.0 Mev using the above calibrated scintillation counter. The cross section has been found to be $(0.898 \pm 0.097) \times 10^{-30}$ square centimeters at a proton energy of 300 kev and $(3.24 \pm 0.35) \times 10^{-30}$ square centimeters at a proton energy of 1.0 Mev.

In presenting this thesis in partial fulfilment of the requirements for an advanced degree at the University of British Columbia, I agree that the Library shall make it freely available for reference and study. I further agree that permission for extensive copying of this thesis for scholarly purposes may be granted by the Head of my Department or by his representative. It is understood that copying or publication of this thesis for financial gain shall not be allowed without my written permission.

Department of Physics

The University of British Columbia,
Vancouver 8, Canada.

Date October 11, 1957

ACKNOWLEDGEMENTS

The author wishes to thank Dr. G.M. Griffiths for his generous assistance with and attentive supervision of the work described in this thesis.

I would like to thank Mr. L.P. Robertson for his kind assistance during the experimental work. Thanks are also due to Mr. P.J. Riley for operation the Van de Graaff during the final part of the work and Mr. G.J. Phillips and Dr. B.L. White for many helpful discussions and suggestions.

Finally, I wish to thank the National Research Council and the Shell Oil Company of Canada for scholarships which have enabled me to carry out this work.

TABLE OF CONTENTS

LIST OF ILLUSTRATIONS

CHAPTER I

INTRODUCTION

A detailed study of the three body systems He^3 and T should lead to a better understanding of the fundamental internuclear forces than is possible from a study of the simpler two body system, the deuteron, since He^3 and T have approximately 2.5 Mev binding energy per particle inferring that the particles are closer together than in the deuteron where the binding energy is only about 1 Mev per particle. Also a comparison of the three body nuclei with the deuteron should, in principle, allow one to determine whether there are many body forces holding the nucleons together in addition to two body forces which are the only ones that can play a role in the deuteron. At the moment such a comparison is not possible because the problem is complicated by relativistic effects of unknown amounts and due to the existence of uncertain non-central components in the binding forces. A theoretical interpretation of the results of the present experiments should give some understanding of the symmetry characteristics of the forces binding the He^3 nucleus together.

The $D(p,\gamma)He^3$ reaction is also of interest to astrophysics since it constitutes an important link in the conversion of hydrogen into helium in the lower temperature main sequence stars by the so-called proton-proton chain. In the lower temperature stars this process predominates over the carbon-nitrogen cycle since the coulomb barriers involved are smaller.

Weak capture radiation from this reaction was first reported by Curran and Strothers (1939). Fowler, Lauritsen and Tollestrup (1949) measured the

angular distribution from a thick ice target at a bombarding energy of 1.4 Mev and found that it had the form $A(\sin^2\theta + \frac{1}{2}b)$ where b was small. They also measured the thick target yield at 90° in the energy range 0.5 Mev to 1.7 Mev giving the total cross section as $\sigma \doteq 0.74\ E^{0.72} \times 10^{-29}\ cm^2$ with a probable error of about 15% in the exponent and of about 50% in the coefficient.

A detailed study of the angular distribution at proton energies of 1.0 Mev and 1.75 Mev was made previously in this laboratory (Griffiths and Warren 1955). The angular distribution was of the form $A(\sin^2\theta + b)$ where b was small and increased as the proton energy decreased from 1.75 to 1.0 Mev and then decreased as the proton energy went below 1.0 Mev. This decrease in b as the proton energy decreased was puzzling theoretically and it was felt that more accurate investigation at lower energies would be of interest.

None of the previous workers were able to give an accurate value for the absolute cross section of the reaction. The present work has attempted to measure the absolute cross section at 0.3 Mev and 1.0 Mev and to make a detailed study of the angular distribution coefficient b in this energy range. In order to do this an accurate measurement of the efficiency of the gamma ray counter and an accurate measurement of the D target thickness was necessary. Measurements were complicated by the $D(d,n)He^3$ reaction since when protons bombard the D target some of the deuterons in the target were elastically scattered and collided with other deuterons producing neutrons by the $D(d,n)He^3$ reaction. The neutrons from this secondary reaction affect the gamma detector and so it was necessary to investigate this effect and to correct for it.

CHAPTER II GAMMA COUNTER EFFICIENCY MEASUREMENT

1. INTRODUCTION

In order to have a scintillation counter of known efficiency for absolute cross section measurements of the $D(p, \gamma)He^3$ reaction the efficiency of a 2.5 inches by 3.5 inches sodium iodide crystal for 6.14 Mev gamma radiation has been measured by simultaneous counting of the alpha and gamma rays from the $F^{19}(p, \alpha, \gamma)O^{16}$ reaction.

The alpha particles which are isotropically emitted are counted in an accurately known geometry. Therefore one can calculate the total number of alphas emitted in the reaction. For each alpha emitted there is a 6.14 Mev gamma ray and therefore one has a gamma source of known intensity which can be used to determine the efficiency of the scintillation crystal as suggested by Van Allen and Smith (1941).

The resonant capture of protons by F^{19} forms Ne^{20} in a highly excited state. This state decays by alpha emission forming O^{16} in the ground state (α_0) or in one of the excited states at 6.06 Mev (α_π), 6.14 Mev (α_1), 6.91 Mev (α_2) and 7.12 Mev (α_3). (Ajzenberg and Lauritsen, 1955). The 6.14, 6.91, and 7.12 Mev states decay by ground state gamma ray emission.

Freeman (1950) has measured the intensity ratios of the short range alphas, (α_1, α_2, α_3) for proton energies between 300 kev and 950 kev obtaining a value of 0.024 for the ratio $\frac{\alpha_2 + \alpha_3}{\alpha_1}$. Chao et al(1950) found that at the 340 kev resonance the ground state group α_0 and the group to the pair emitting state α_π, were not experimentally observable. They also noted that the total number of alpha particles was closely equal to the total number of gamma rays at the resonances measured. The experimental

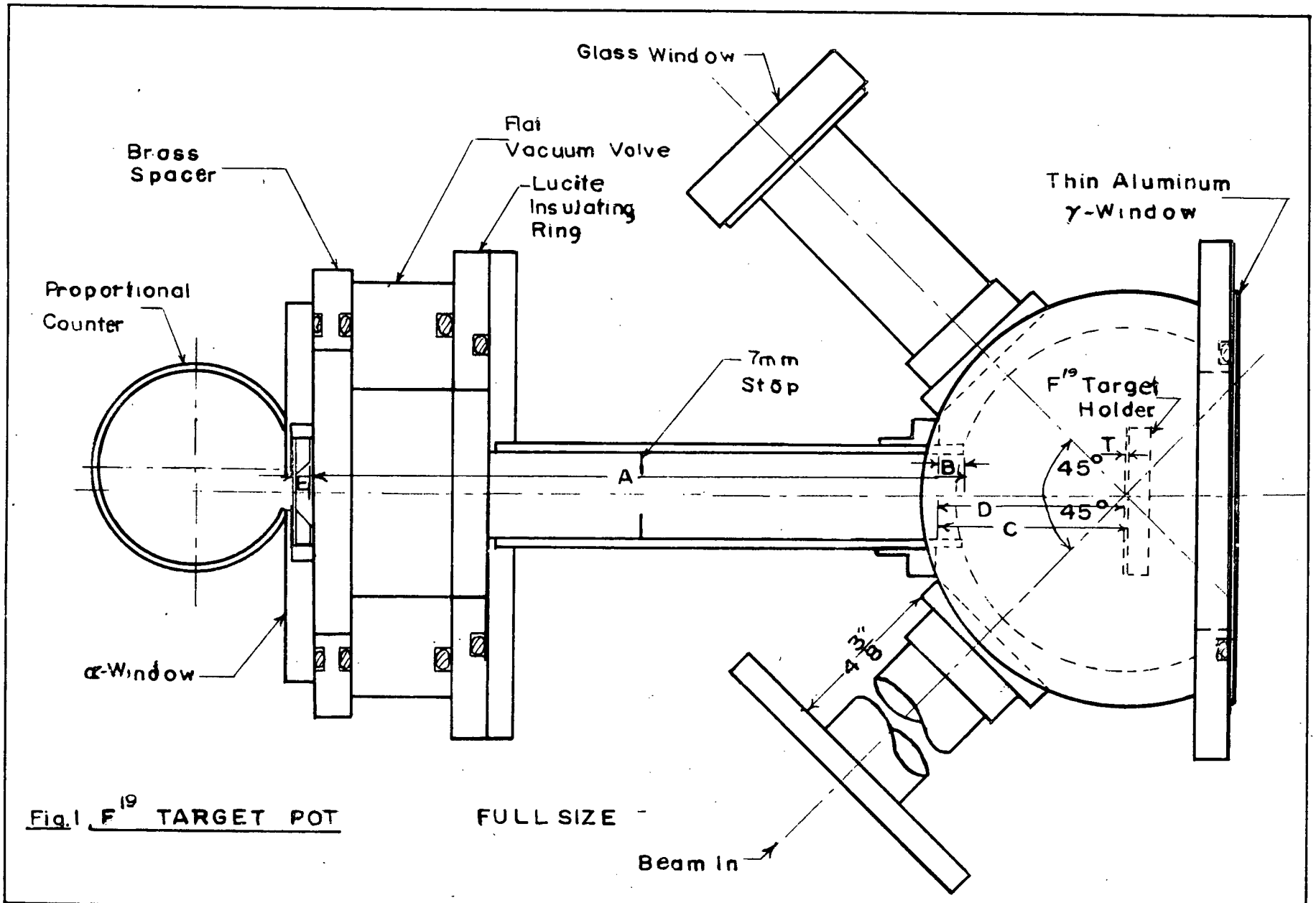

Fig. 1 F^{19} TARGET POT FULL SIZE

results of Devon and Hine (1949) and the spin assignments of Chao (1950) show that the alpha particles and gamma rays are isotropically distributed at the 340 kev resonance.

H. Dosso (1957) in this laboratory has measured the relative intensities of the 6.14 Mev gamma ray and the sum of the yields of the 6.91 and 7.12 Mev gamma rays with a four crystal spectrometer. He gives 2.3% $\pm$ 0.2% as the ratio of 6.91 Mev plus 7.12 Mev to the 6.14 Mev gamma rays. This result is in very good agreement with the value of 2.4% as found by Freeman from relative alpha particle intensity measurements.

Van Allen and Smith (1941) used a variable pressure absorption cell ionization chamber as an alpha counter and a thin-ended geiger counter for the gamma rays. In the present work the alpha particles were counted by a gas proportional counter sensitive only to the 6.14 Mev state alpha particles. From the known solid angle the total number of alpha $\overset{\circ}{\lambda}$ emitted by the source could be calculated and this corresponds to the total number of 6.14 Mev gamma rays emitted by the source. The total number of gamma rays was assumed to be equal to the total number of 6.14 Mev gamma rays plus 2.3% to allow for the 6.91 and 7.12 Mev gamma rays for which the alpha particles had insufficient energy to enter the proportional counter. The details of the counters are described below.

2. APPARATUS

(a) The $F^{19}(p,\alpha,\gamma)O^{16}$ Target Chamber

The target chamber used in this experiment is shown in Fig. 1.

The alpha particle counter was attached to the middle of the three brass tubes of the chamber. This tube had a brass stop located so as to prevent small angle alpha scattering.

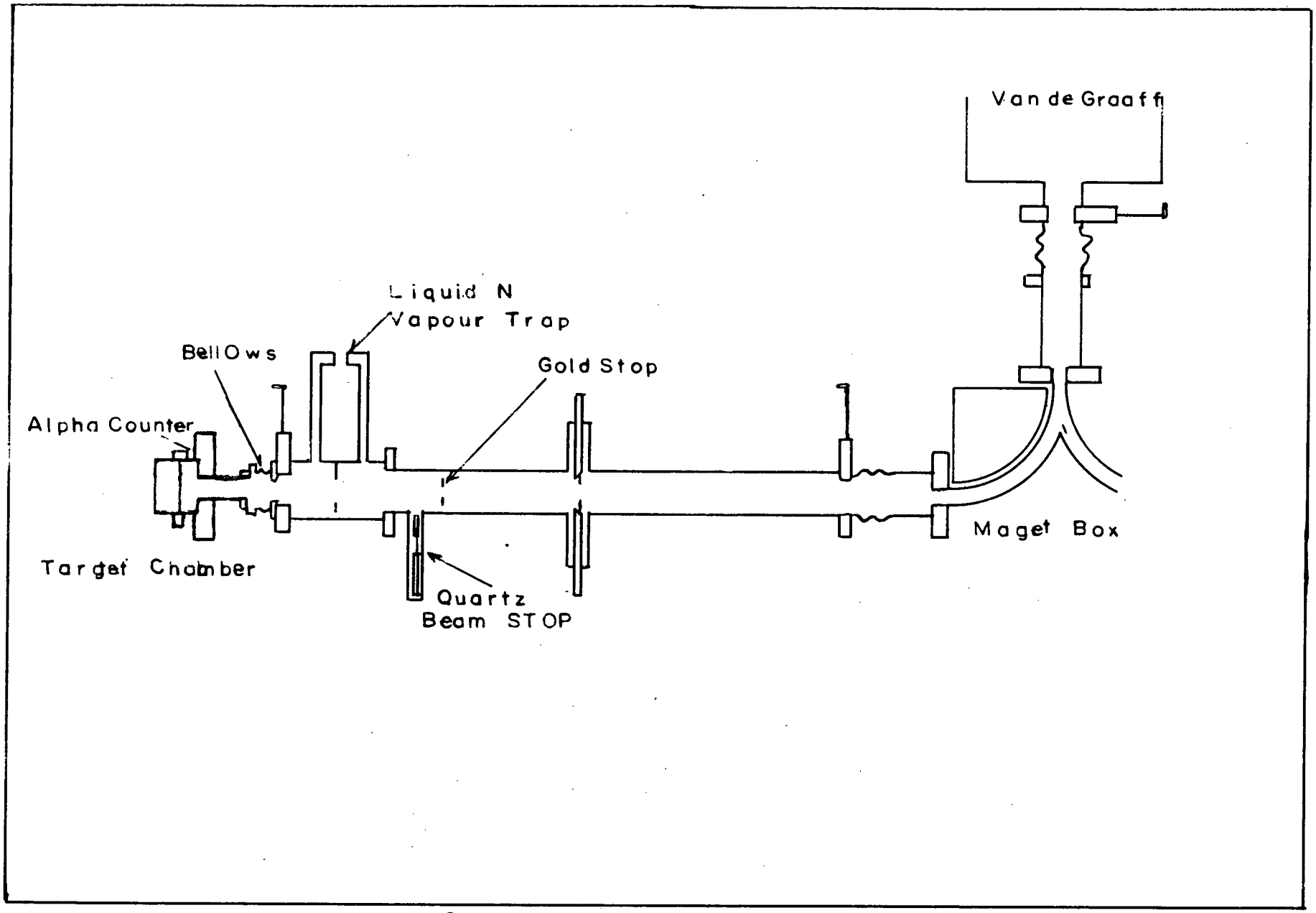

Fig. 2 Beam Tube

The target chamber was aligned using the viewing tube with the glass window in the following manner. The target was rotated so that the polished back was at an angle of 45° to the beam tube. A light shining into the beam tube could be seen through the beam stops reflected on the target backing. The target chamber was then adjusted by moveable bellows until it was concentric with a stop in the main Van de Graaff beam tube. Any further alignment was done so as to maximize the current on the target and to minimize that scattered in the beam tube.

The target plate was bolted onto a copper frame which was electrically insulated by lucite spacers from the outer chamber. The frame could be rotated for replacement of targets. The experiments were done with the target at 45° to the beam so that the alpha particles came through a minimum thickness of calcium fluoride. The gamma ray counter "looked" at the back of the target. The absorption of the gamma rays by the 0.029 inch thick aluminium window was about 0.5% and by the 0.015 inch thick copper target backing was about 0.9%. The gamma ray yield was corrected for this absorption.

A liquid nitrogen vapour trap was used in front of the target chamber to prevent carbon from the oil diffusion pumps of the main vacuum system being laid down on the target. See Fig. 2. Molybdenum and gold stops were used in the beam tube as shown as those materials produce very little background.

A magnetically controlled quartz beam stop was used to cut the beam from the target except when runs were being made.

(b) Fluorine Targets

The targets were prepared from powdered calcium fluoride evaporated in a bell jar under vacuum on to thin copper plates. The calcium fluoride was

weighed before evaporation and the distances between the boat and the copper sheets measured so that targets could be reproduced. For example, in one particular evaporation 0.031 gm of calcium fluoride produced on a sheet of copper 25 cm above the boat a target of three kev thickness for 340 kev protons. The target thickness was approximately inversely proportional to the square of the distance from the boat.

The targets were inspected visually for uniformity and any non-uniform ones were discarded. The shape of the excitation curve was also noted during the experiments and any nonuniformity of the targets was shown by the asymmetry of the curve. Some targets, especially those used for the high beam current trials, showed blistering from the heating effect of the beam. Targets were changed frequently during the experiment to prevent their deterioration.

(c) Counters

(i) Gamma Ray Counter

The scintillation crystal which was calibrated is a Harshaw Thallium activated sodium iodide srystal. Its dimensions, as supplied by Harshaw, are 2.500 ± 0.005 inches diameter by 3.500 ± 0.005 inches long. The crystal was mounted by Harshaw in an aluminum can with magnesium oxide reflector.

The photomultiplier tube was a Dumont No. 6363 with a 2-5/8 inch diameter photocathode surface. The crystal was held on to the photomultiplier tube by a vulcanized rubber band. Dow Corning 200,000 centistoke Silicone oil was used to ensure good optical coupling between the crystal and the photomultiplier tube.

The crystal and photomultiplier together with the preamplifier were all mounted inside a 3-3/8 inch brass tube approximately fifteen inches long. The

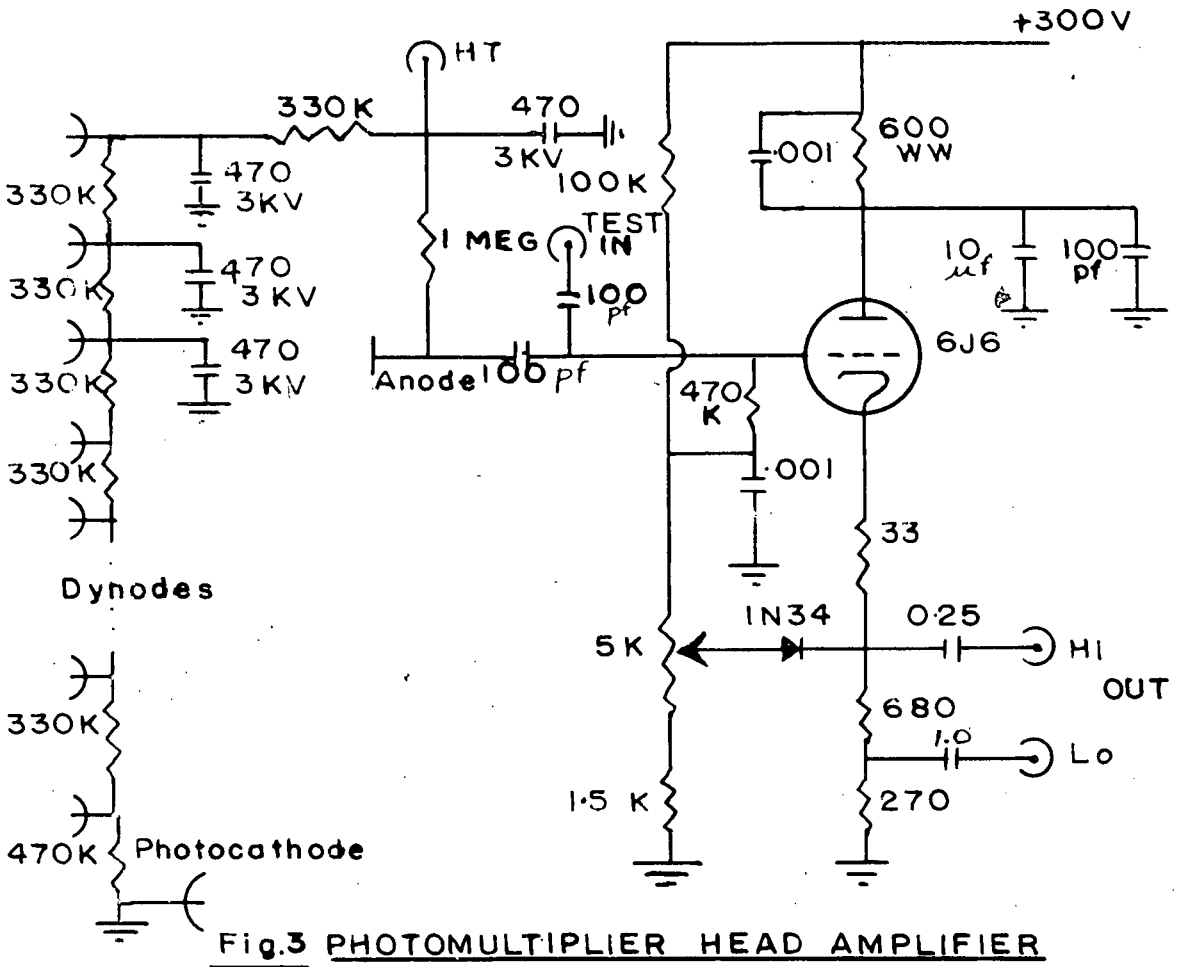

Fig.3 PHOTOMULTIPLIER HEAD AMPLIFIER

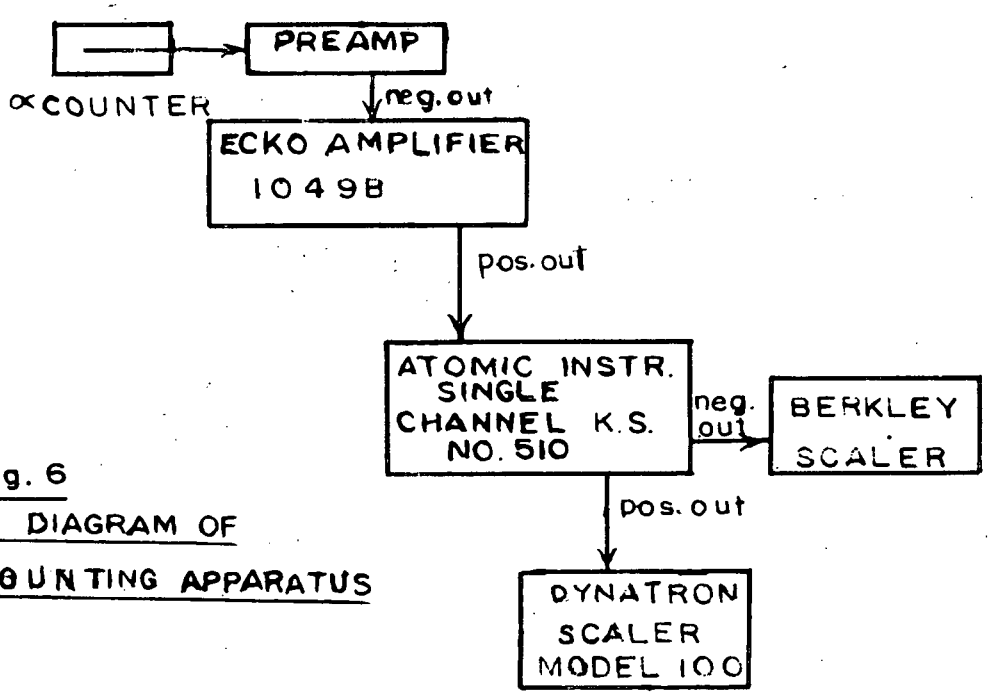

Fig. 6

BLOCK DIAGRAM OF

∝ COUNTING APPARATUS

counter is shown in Plate 1. The single cyclindical unit made precise levelling and positioning of the counter as described later relatively easy. A mu metal shield was put around the photomultiplier tube to shield it from the field of the Van de Graaff's main magnet.

The preamplifier, mounted inside the brass tube, was a 6J6 cathode follower. The circuit diagram is given in Fig. 3.

This scintillation counter has now operated well for a year with no noticeable change in its energy resolution. A resolution of about seven per cent for the photo-peak of the 2.62 Mev RdTh gamma ray has been obtained.

(ii) The Alpha Particle Counter

The alpha counter was attached to the target chamber as shown in Fig. 1. The proportional counter is a stainless steel tube 1.5 inches in diameter and five inches long. It is filled with eleven cm of argon and one cm of alcohol. The counter size and gas pressure was chosen so that the alpha particles associated with the 6.14 Mev gamma rays of the reaction would stop in the gas of the counter.

The counter has a 6.1 mm air equivalent mica window cemented as shown in Fig. 4. This window thickness was chosen so as to stop all scattered protons from the target and as a result it also stops the 6.91 and 7.12 Mev state alpha particles from entering the counter. The 6.14 Mev state alpha particles with an initial energy of 1.85 Mev pass through the window with an energy of about 0.7 Mev.

The counter body is offset from the center of the entrance aperture so that alpha particles would not hit the centre wire. The centre wire is 0.005 inches in diameter made of a copper-nickel alloy and was diamond drawn to ensure uniformity along its entire length. For the precise

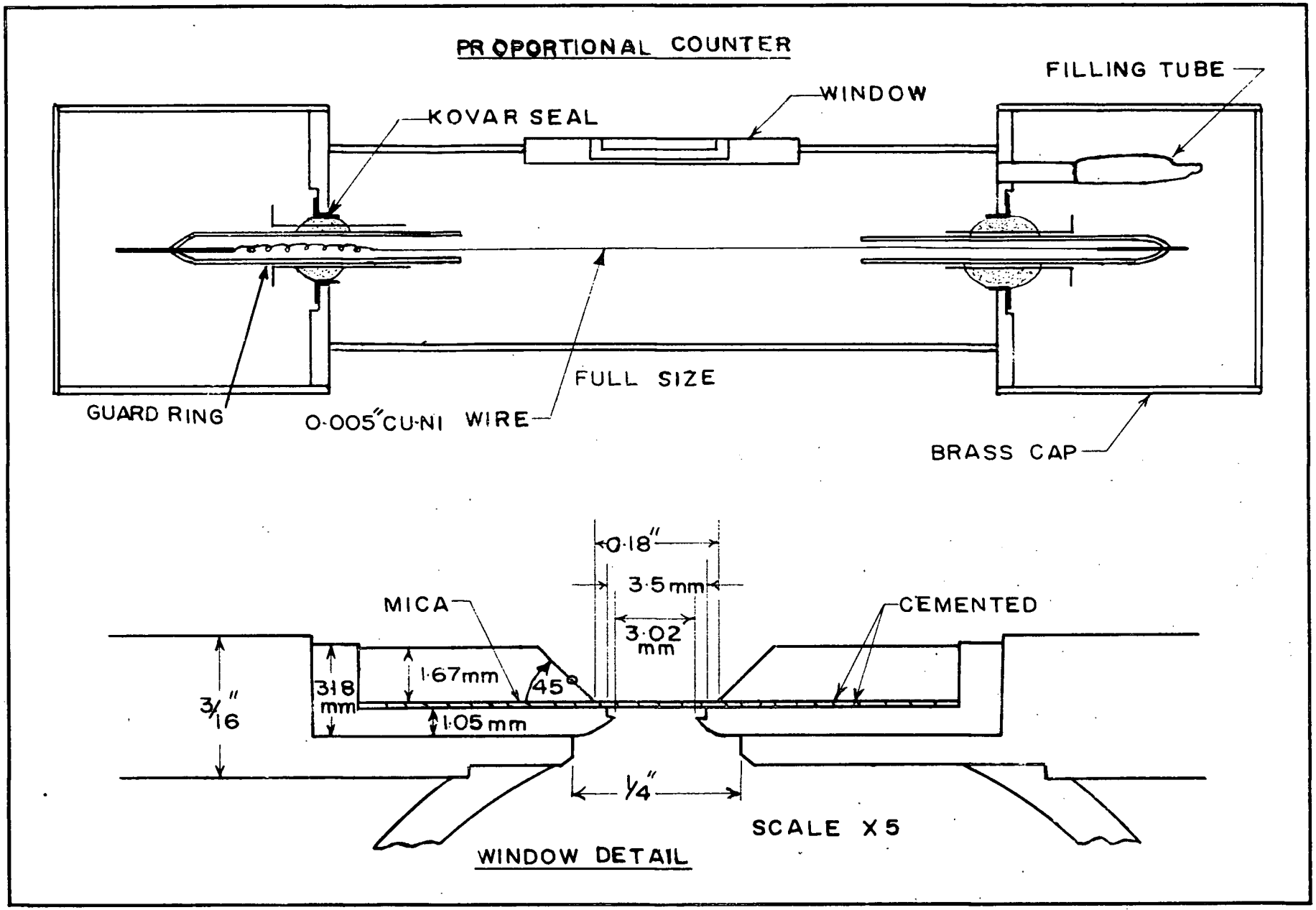

Fig. 4 Alpha Partile Counter

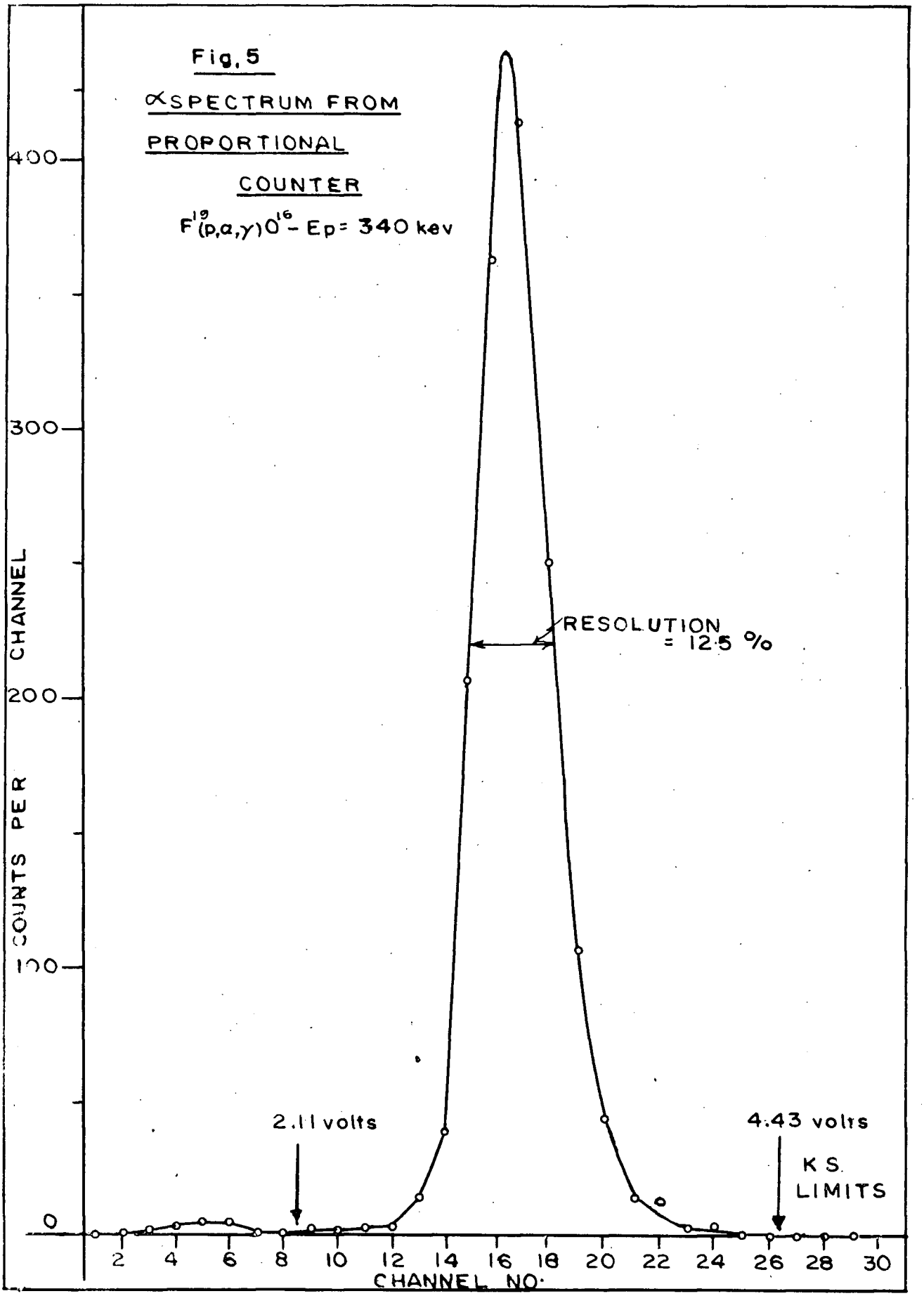
Fig. 5
∝ SPECTRUM FROM PROPORTIONAL COUNTER
$F^{19}(p,\alpha,\gamma)O^{16}$ - Ep = 340 kev
COUNTS PER CHANNEL
400
300
200
100
0
RESOLUTION = 12.5 %
2.11 volts
4.43 volts
K.S. LIMITS
2 4 6 8 10 12 14 16 18 20 22 24 26 28 30
CHANNEL NO.

calibration of the NaI crystal it was essential that the solid angle of the alpha counter be well defined. The entrance window is shown in Fig. 4. The entrance aperture dimensions and the counter to target distances shown in Fig. 1 were all accurately measured.

A "flat" vacuum valve was between the counter and the target chamber arm. This valve was opened only when the target tube had been evacuated. In this way the mica window was protected from atmospheric pressure when the counter was not in operation.

The proportional counter centre wire was operated at a potential of 800 volts which gave a gas multiplication factor of ten. The guard rings which define the sensitive volume of the counter were at the same voltage as the centre wire.

A typical alpha particle spectrum is shown in Fig. 5. A resolution of 12.5% was obtained for the alpha particle group associated with the 6.14 Mev gamma ray of the fluorine reaction.

(d) Electronic Counting System

A block diagram of the alpha particle counting system is shown in Fig. 6. Negative pulses from the alpha - counter were fed via a 6AK5 cathode follower into an E.K. Cole Model 1049 B amplifier. Positive pulses from this unit were put into an Atomic Instruments Single Channel Pulse Height Analyzer Model 510. The single channel "kicksorter" window was set to give out only those pulses in the 1.85 Mev alpha particle peak corresponding to the 6.14 Mev gamma ray as shown in Fig. 5.

The positive output pulses from the window were fed into a decade scaler. The negative output from the base line discriminator was fed into a Dynatron Model 100 scaler. In this way a record was kept of all alpha pulses

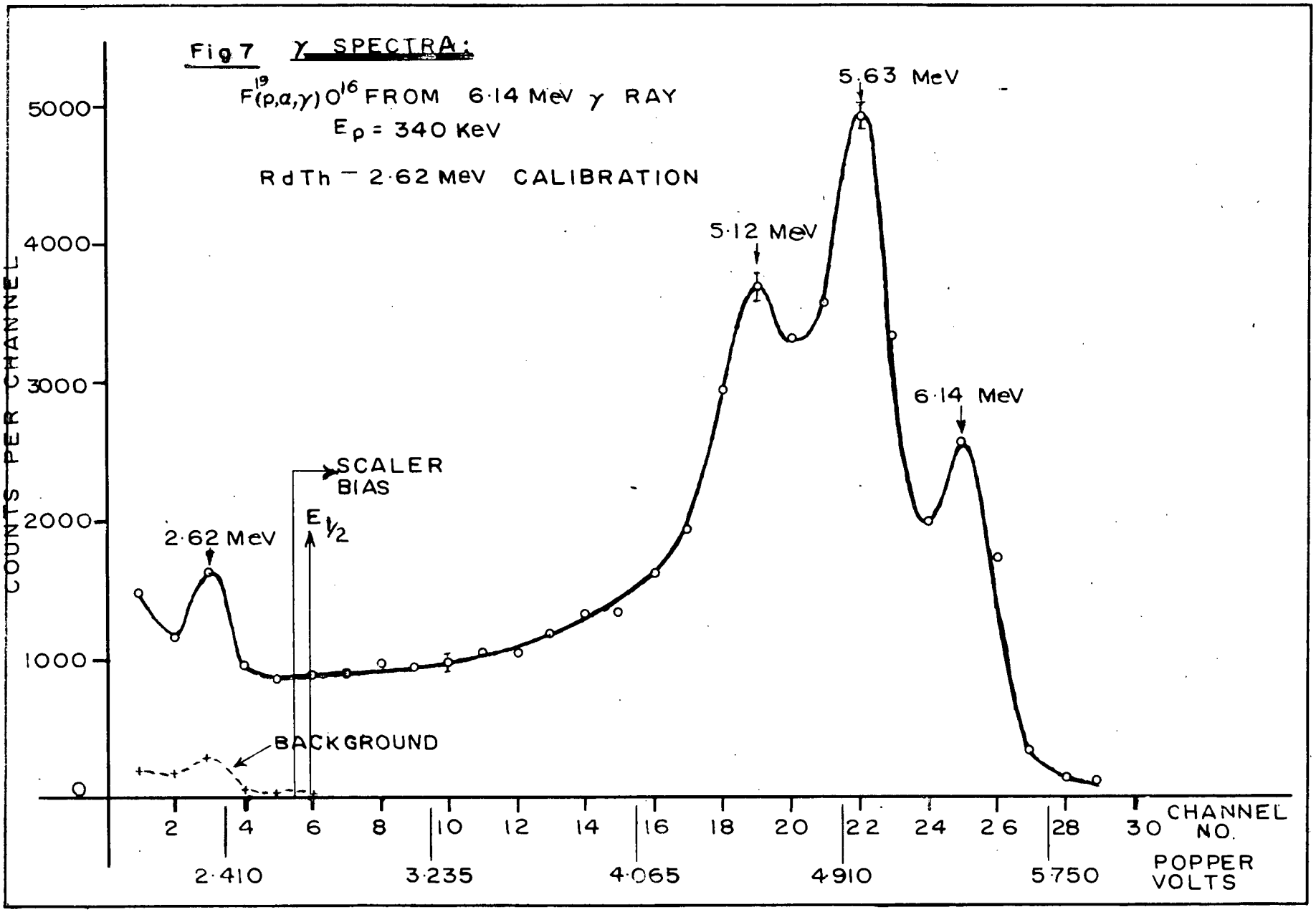
Fig 7 γ SPECTRA:
$F^{19}(p,\alpha,\gamma)O^{16}$ FROM 6·14 MeV γ RAY
E_p = 340 KeV
RdTh — 2·62 MeV CALIBRATION
5·63 MeV
5·12 MeV
6·14 MeV
2·62 MeV
SCALER BIAS
$E_{1/2}$
BACKGROUND
COUNTS PER CHANNEL
5000
4000
3000
2000
1000
0
2 4 6 8 10 12 14 16 18 20 22 24 26 28 30
CHANNEL NO.
2·410
3·235
4·065
4·910
5·750
POPPER VOLTS

above the lower edge of the window.

The scintillation counter high voltage was supplied by an Atomic Instruments Superstable Power Supply set at 1080 volts. The negative pulses from the cathode follower were fed into a Northern Electric Model No. 1444 amplifier.

The discriminator output of this amplifier was put into a Dynatron Scaler. The bias voltage was set to be just below the half energy point of the fluorine gamma ray as shown in Fig. 7. The negative output pulses from the amplifier were fed via a biased amplifier into a thirty channel Marconi Pulse Amplitude Analyser ("kicksorter.")

The biased amplifier was set so that the 6.14 Mev gamma ray was near the top of the kicksorter while the 2.62 gamma ray of RdTh was in the bottom channels. Thus a direct energy calibration was available from which the half energy point of the 6.14 Mev gamma ray was determined. A typical spectrum is shown in Fig. 7.

Gain shifts or nonlinearities in the electronic system was checked using a mercury relay pulse generator described by Robertson (1957). Test pulses were put directly on the grids of the counter's cathode follower. The channel edges of the kicksorter were set from these pulses through the scintillator counter preamplifier. In this way any non-linearity in the amplifier-kicksorter system was eliminated.

The single channel kicksorter limits for the alpha peak were set in the same manner by test pulses fed into the alpha counter head amplifier.

3. EXPERIMENTS

The University of British Columbia's Van de Graaff Generator provided

a well-stabilized beam of up to ten microamperes of protons on the fluorine target.

An excitation curve was first done over the 340 kev resonance of the F^{19}. The position of the resonance on the generating voltmeter scale was obtained. The shape of the excitation curve also gave a check on the uniformity of the fluorine target.

If the target was satisfactory the scintillation crystal was levelled, set at the same height as the beam spot and set perpendicular to the target. A trial at any one position was broken into separate runs. The spectra was recorded each time so that a check was kept on the stability of the equipment. RdTh calibration runs were made at each position. Time and beam dependent backgrounds were taken so that corrections could be applied in the calculations.

The time taken for runs at any one position was set by the necessity of obtaining one percent accuracy in the counting statistics. This required about ten thousand counts in the alpha and gamma spectra.

At the two closest distances the gamma ray counting rate was extremely fast unless a proton current of less than two micro-amperes was used. It was found that the gain of the Dumont photomultiplier used on the gamma counter tended to shift with a count rate of about 1500 counts per second or above. This shift was observed with the accurate test pulse generator feeding pulses directly into the counter head amplifier. After counting at a high rate the position of the spectrum changed while the voltage levels on the kicksorter and the amplifier gains remained constant, thus confirming that the photomultiplier gain had shifted. The gain increased with high counting rate and amounted to a 0.3% change when the high counting rate was

maintained for about thirty minutes. This gain shift had a slow decay time returning gradually to its original value after a few hours.

4. CALCULATIONS

The proportional counter records only the 6.14 Mev state alpha particles. The gamma spectrum, however, contained the 6.14, 6.91, and 7.12 Mev gamma ray yields. The sum of the 6.91 and 7.21 Mev yield is 2.3% (Dosso 1957) of the total yield at 340 kev. The spectra were corrected so that only the gamma counts from the 6.14 Mev state were considered in the calculations.

The change in cross section of sodium iodide for gamma rays of 7.12 and 6.14 Mev is approximately 0.004% and was therefore neglected in the calculations.

The RdTh and the F^{19} spectra were plotted as in Fig. 7. Knowing the position and energy of these peaks the half energy point of the 6.14 Mev gamma ray was calculated.

The kicksorter channel readings were summed from the half energy point and corrected for the 2.3% of the 6.91 and 7.12 Mev radiation. The background was normalized to the duration of the run since the background contributed by the beam alone in the 6 Mev region was almost zero. See Fig. 7.

The number of 6.14 Mev gamma counts were corrected for the 0.3% absorption in the aluminium window and the 0.9% absorption in the copper target backing.

The alpha counter background was about .3% of the number of alpha counts obtained in the same time with about two microamperes on the target. The square root of the ratio of the alpha counts to the gamma counts was calculated for each of eight positions of the gamma counter and the graph

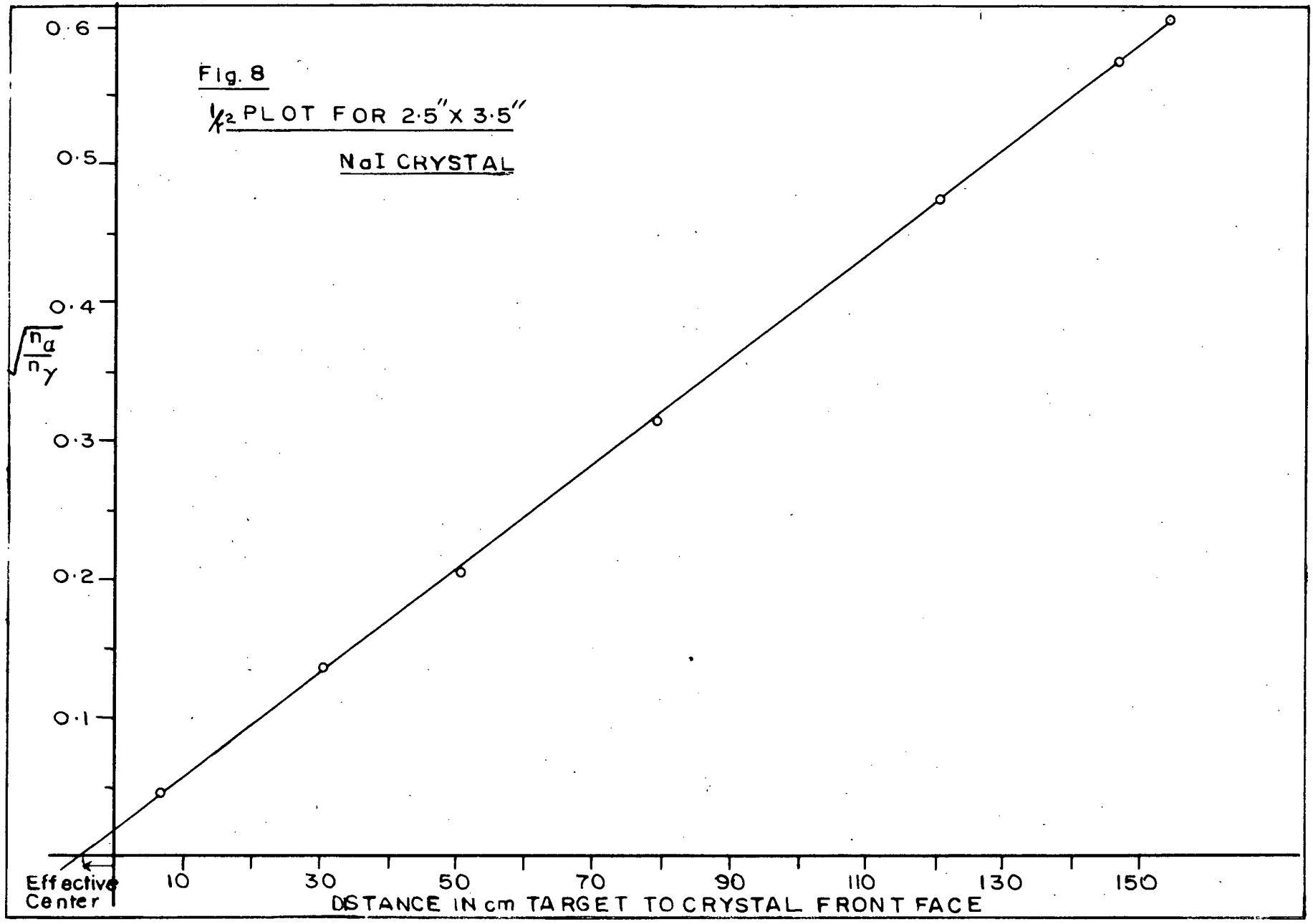
Fig. 8
1/r² PLOT FOR 2.5" X 3.5"
NaI CRYSTAL
0·6
0·5
0·4
0·3
0·2
0·1
√(n_a/n_γ)
Effective Center
10
30
50
70
90
110
130
150
DISTANCE IN cm TARGET TO CRYSTAL FRONT FACE

of Fig. 8 plotted. This line, extrapolated to zero, gives the effective center of the crystal at 4.22 ± 0.23 cm from the front face of the crystal.

Solid Angle Calculations:

(a) Alpha particle counter: -

Referring to Fig. 1, the dimensions are as follows: -

$A = 4.8130 \pm 0.0010$ inches

$B = 0.1766 \pm 0.0013$

$C = 1.4165 \pm 0.0009$

$E = 0.087 \pm 0.003$

$t = 0.0152 \pm 0.002$

Total distance from target to center of window defining aperture -

$$R = A + C + E + B + t$$

$$= 6.1247 \pm 0.0082 \text{ inches}$$

The alpha counter window was measured across many diagonals by two travelling microscopes. Since all the readings were approximately the same the mean diameter was taken as 3.020 ± 0.002 mm.

The solid angle of the alpha counter is thus: -

$$\omega_\alpha = \pi \left(\frac{3.020}{2 \times 6.1247 \times 25.400} \right)^2$$

$$\omega_\alpha = 2.956 \times 10^{-4} \text{ ster-radians}$$

(b) Gamma Ray Counter: -

Diameter of crystal 2.500 ± 0.005 inches

$$\text{Area} = \pi \left(\frac{2.500}{2} \times 2.54 \right)^2$$

$$A_\gamma = 31.67 \text{ cm}^2$$

Effective Solid Angle of counter -

$$\omega_\gamma = \frac{31.67}{(D + 4.22)^2}$$

Where D is the distance from the target spot to the crystal face.

Efficiency:

The efficiency of the crystal was calculated for each distance from the target.

$$\text{Crystal Efficiency} = \frac{(\text{No. } \gamma\text{-counts above } E_{\frac{1}{2}})\ (\text{solid angle of } \alpha\text{-counter})}{(\text{No. of } \alpha\text{-counts})\ (\text{solid angle of } \gamma\text{-counter})}$$

$$\epsilon = \frac{n_\gamma \quad \omega_\alpha}{n_\alpha \quad \omega_\gamma}$$

5. Results:

The results, together with their estimated errors are given in the following table.

Table I

D + 4.22 ± 0.23 cm.		EFFICIENCY	ERROR
154.52	± 0.28 cm	0.6179	± 1.35%
146.82	0.28	0.6146	1.35
120.47	0.30	0.6120	1.35
79.22	0.30	0.6067	1.45
51.47	0.30	0.6105	1.64
33.95	0.28	0.6124	2.04
20.32	0.28	0.6466	2.96
11.72	0.25	0.6433	5.35

Efficiencies of NaI Crystal

The error is estimated from the counting statistics

$$\Delta n_\alpha = \sqrt{n_\alpha} \quad , \qquad \Delta n_\gamma = \sqrt{n_\gamma}$$

the percentage uncertainty in the measurement of the distances from the alpha counter aperture to the target and the uncertainty in the distance of gamma counter effective center to the target $\left(\frac{\Delta r_\alpha}{r_\alpha} \ , \ \frac{\Delta r_\gamma}{r_\gamma} \right)$ and percentage uncertainty in the area of the alpha counter window. Thus the estimated error in the efficiency is:

$$\Delta \epsilon = \sqrt{\left(\frac{\Delta n_\gamma}{n_\gamma}\right)^2 + \left(\frac{\Delta n_\alpha}{n_\alpha}\right)^2 + \left(\frac{\Delta r_\gamma}{r_\gamma}\right)^2 + \left(\frac{\Delta r_\alpha}{r_\alpha}\right)^2 + \left(\frac{\Delta A_\alpha}{A_\alpha}\right)^2}$$

The mean of the first five values is 0.612 ± 0.009.

The larger estimated error in the last three values is due mainly to the uncertainty in the position of the effective center of the crystal.

The last value in the table has an uncertainty of three per cent in the alpha counting statistics since about one thousand alpha counts were taken

in this run while about ten thousand counts were taken in the rest of the trials. The total 6.14 Mev gamma counts ranged from about thirty thousand to over two million. As stated previously the gamma counting rate at the short target to counter distances was extremely fast. Therefore a low beam current was used which made the alpha particle yield very small. The one thousand alpha counts of the last trial took several hours of machine operating time. In conclusion the absolute efficiency of the scintillation counter for 6.14 Mev gamma rays is 0.612 $\pm$ 0.009.

H. Dosso (1957) and P. Singh in this laboratory have measured the absolute efficiency of this counter for the Co^{60} gamma rays of 1.33 and 1.17 Mev. P. Singh has carried out theoretical calculations the results of which agree with the Co^{60} measurements within the accuracy of the source strength calibration done by the National Research Council.[1] Singh has also calculated the efficiency for 6.14 Mev gamma rays which agrees to within five per cent with the results of the present work.

Due to the good agreement between the theory and the experimental observations at one and six Mev it would appear that the theoretical estimate of the efficiency between one and eight Mev should be accurate within five percent, particularly if the theoretical calculations are adjusted to fit the experimental value at 6.14 Mev which is accurate to 1.5%. In determining the absolute cross section for the $D(p,\gamma)\ He^3$ reaction

---

1 This source was calibrated by National Research Council, Report No. APXNR - 325. The strength was given as 0.178 $\pm$ 0.007 milliroentgens per hour at 1 meter (0.134 $\pm$ 0.005 mc.) scintillation counter comparison with a Co^{60} source giving 1.39 $\pm$ 0.05 milliroentgens per hour at one meter. The latter source was measured by ionization chamber comparsion with the Canadian primary radium standard (N.R.C. Report No. C-121).

the efficiency is required for gamma rays in the range 5.7 Mev to 6.2 Mev. The efficiency over this energy range has been extrapolated from the experimental value at 6.14 Mev on the basis of the theory.

CHAPTER III D_2O ICE TARGET THICKNESS MEASUREMENTS

1. INTRODUCTION

The absolute cross section measurements of $D(p, \gamma) He^3$ reaction to be described in Chapter IV required that the thickness of the heavy ice target be measured.

This thickness was measured by noting the shift of the 340 kev proton resonance of fluorine caused by the protons travelling through the ice layer. The number of D_2O atoms per sq. cm was then calculated using the measurements of the stopping power of D_2O ice for protons. Wenzel and Whaling (1952) measured, with an accuracy of four per cent, the stopping cross section of D_2O ice for protons between 18 kev and 541 kev. Their results agree within experimental errors with the theoretical calculations of Hirschfelder and Magee (1948) for energies greater than 300 kev.

From the experiments described below a calibration curve for the D_2O dispenser has been obtained for target thicknesses from 30 kev to 110 kev for 340 kev incident protons.

2. APPARATUS

(a) Target Chamber

The target chamber, shown in Plate 1, was of a type used before in this laboratory (Griffiths and Warren 1955). The ice target backing was a copper plate 7/8 inch by 1 inch and 1/16 of an inch thick. The copper plate was soldered to a brass liquid nitrogen trap which was

electrically insulated from the outer container by a lucite ring. The target was operated at +135 volts to suppress secondary electrons and thereby prevent erroneous beam current readings.

The adjustable bellows used in the efficiency measurements was also used on the front of this chamber. A lucite ring electrically insulated the beam tube from the bellows. Thus the amount of beam current striking the beam tube could be measured. This was of great assistance in the rather critical alignment necessary with this chamber. Molybdenum stops with 6 mm and 8 mm aperture were put in the beam tube to reduce scattering of the incident beam onto the target. A degree circle was attached to the bottom of the outer chamber so that horizontal angles could be read during the angular distribution measurements.

A liquid nitrogen vapour trap was used between the target chamber and the main vacuum system of the Van de Graaff. It had a copper stop with a one inch hole through which the beam passed. This trap was always removed from the beam tube at the end of the runs while it was still cold. In this way D vapour frozen onto the trap was kept out of the main vacuum system. Any D in the system would have added greatly to the beam dependent background. There was no noticeable increase in beam dependent background during this series of experiments.

A magnetically controlled quartz stop was used to keep the beam from the D target except when readings were being taken.

(b) D_2O Dispenser

The D_2O dispenser shown in Plate 1 was made of glass. Its

three taps had been individually ground so that a vacuum tight fit was ensured. The dispenser was mounted on plywood so that it could be attached by a bracket to the target chamber. A piece of centimeter graph paper was cemented behind the monometer. The level of the oil in the U-tube was read directly from this scale.

Oil was chosen as the indicating fluid. Mercury had previously been used in this laboratory. However, with a density of 0.9 gm/cc., oil has about fifteen times greater sensitivity than mercury. Octoil Vacuum Pump Fluid from Distillation Products Industries with a vapour pressure of 10^{-7} mm mercury at 20° C. was used.

The oil was heated under vacuum to remove water and other volatile impurities. Both the oil and the dispenser were pumped for two days to remove all volatile vapours. About forty cc. of oil were put in the dispenser U-tube. This allowed the full vapour pressure of D_2O at room temperature (about 24 cm) to be measured on the monometer. The top glass tube of the dispenser fitted into an O-ring joint on the outer target chamber.

(c) Scintillation Counter

The scintillation counter whose efficiency was measured in Chapter II was used to count the gamma rays. It was set at 90° to the proton beam and was shielded by two inches of lead on the top and at the sides to cut down background radiation.

Negative pulses from the head amplifier of the scintillation counter

were put into a Northern Electric Model No. 1444 amplifier. The discriminator output of this amplifier was fed into a Tracerlab Inc., Model SC-34A count rate meter. The discriminator bias of the amplifier was set just above the 2.62 Mev RdTh peak since a large percentage of the room background was due to thorium in the concrete of the walls and floor.

3. EXPERIMENT

Fluorine targets of thicknesses between three and ten kev were prepared as described in Chapter II. The copper sheets were indium coated on the backs before the fluorine evaporation. After preparation they were soldered onto the copper target plate described above using low melting point (155° C) indium so as not to disturb other soldered joints.

As the runs were made a careful check was kept on the excitation curves. Asymmetry of the excitation curve would have indicated a non uniform target. Targets were changed when any deterioration was noted. A low proton current of less than two microamperes was used for these experiments. In this way deterioration of the heavy ice layer was kept at a minimum.

After the fluorine target had been soldered into place and the target chamber and monometer allowed to pump down as low as possible the dispenser was shut off by the top tap. The target chamber was rotated until the fluorine target was facing and perpendicular to the dispenser inlet. The inner pot was filled with liquid nitrogen. The dispenser tap connecting the two arms of the U tube was closed. The lower tap was opened allowing a suitable amount of vapour as indicated by the oil levels to enter the

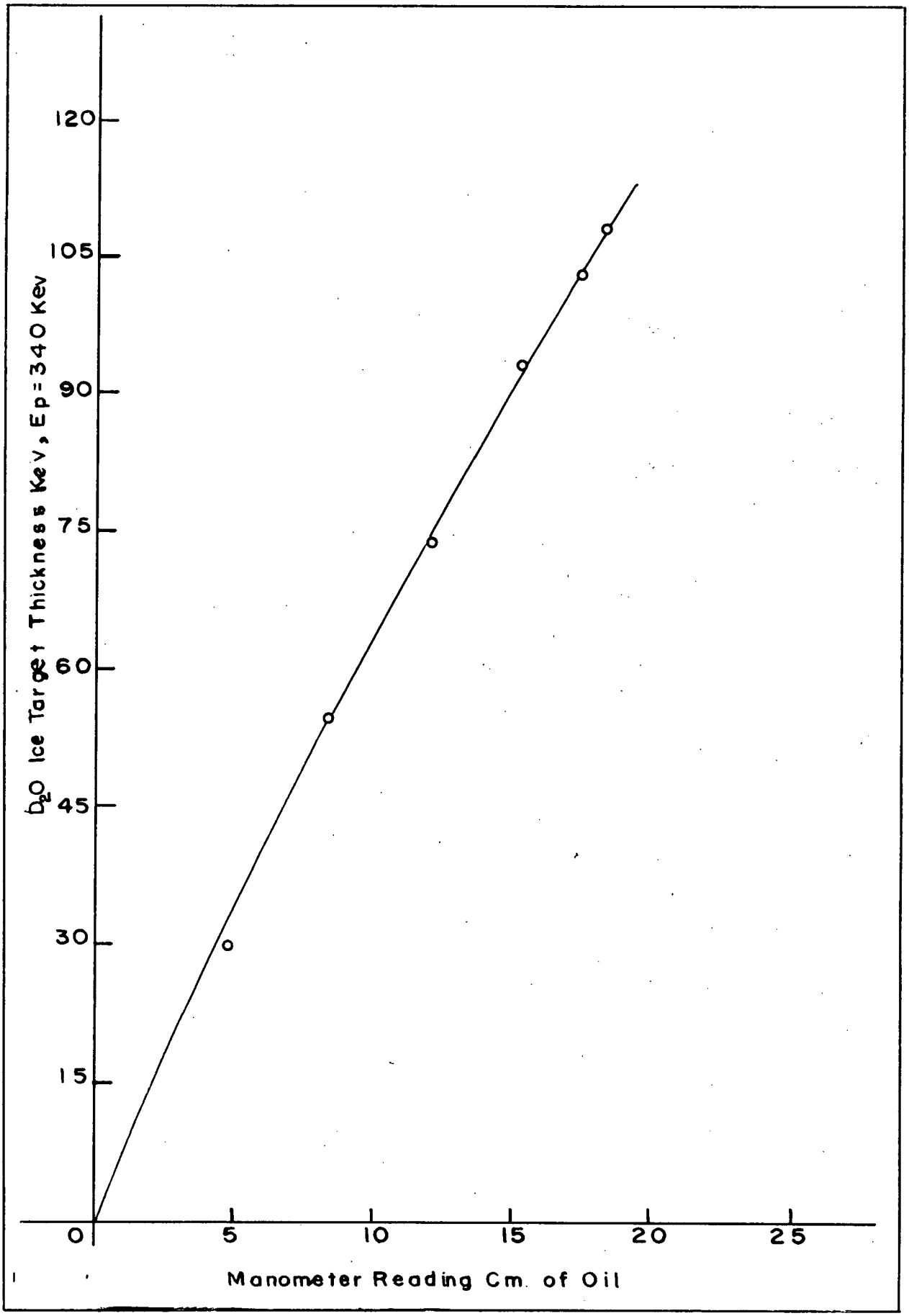

Fig. 9 D_2O Dispenser Calibration Curve

enclosed volume. The oil levels were recorded. The top tap was slowly opened and the vapour was pumped out of the dispenser through a brass rod which had a 1/16 inch diameter hole drilled through it. The vapour then diffused through a 1/8 inch thick glass wool plug held by a copper screen and sprayed out, freezing over the fluorine target. After the oil levels had come back to their original positions the tap was closed.

The above procedure was repeated in a standard manner for each heavy ice target with reproducible results. A uniform spot about 1.5 cm in diameter was formed on the target plate.

After each of the calibration trials the ice target was removed and a resonance check made on the bare fluorine target.

4. RESULTS

The calibration graph is shown in Fig. 9. Fig. 10 shows the readings for one particular trial. The first curve is the excitation curve for the bare fluorine. The resonance peak is at 338 kev as measured on the Van de Graaff generating voltmeter scale. An ice target corresponding to 12.10 $\pm$ .05 cm of oil was put on top of the fluorine and a second excitation curve done with the protons passing through the ice layer. The resonance had shifted to 412 kev as shown in the second curve of Fig. 10. This indicates that a change of 12.10 cm on the oil monometer gives a target thickness of 74 kev as shown on the graph.

The calibration was not carried out far beyond a 100 kev thickness, since for the absolute yield measurements the maximum target thickness required was 100 kev for 300 kev incident protons.

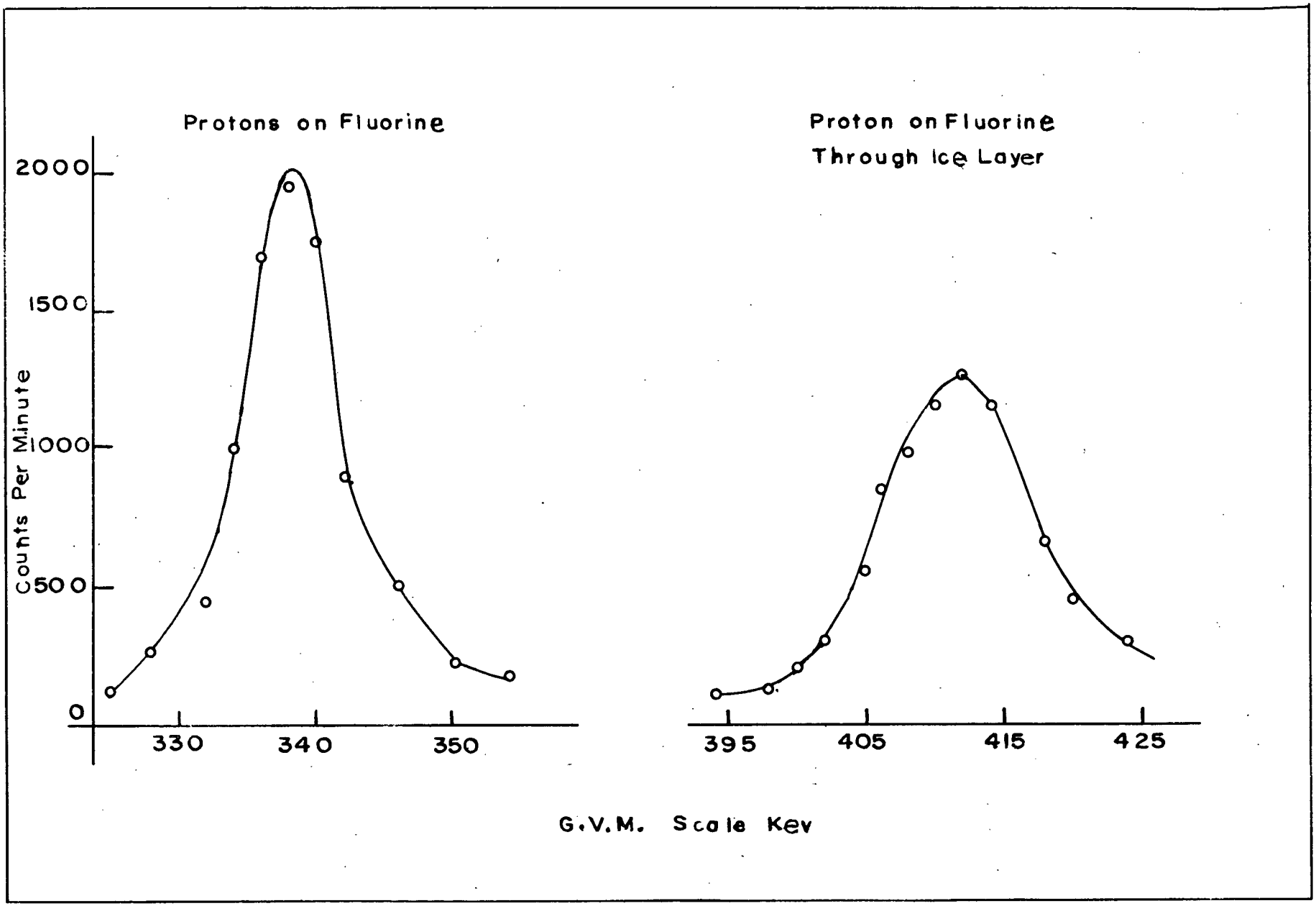

Fig. 10 D_2O Ice Target Thickness Calibration

It will be noticed from Fig. 10 that the resonance curve taken with the ice layer on the fluorine is lower and broader than the one taken on the bare fluorine. The full width at half height has, in fact, increased from 7.5 to 14 kev. The width of the first curve is contributed by the width of the fluorine resonance, the thickness of the fluorine target and the proton beam energy spread. These effects give a width of 7.5 kev as seen from the bare fluorine measurement. The increased width from the protons passing through the ice is due to straggling of the protons in the ice and to non-uniformities in the ice target.

Since the integrated areas of the two curves are approximately the same the centers of the curves were taken as the resonance peak and the dispenser calibration graph was obtained on this basis.

The thickness of the targets in atoms per sq. cm. was calculated in the following manner using the results of Wenzel and Whaling (1952).

$$n_D \text{ atoms } /cm^2 = \frac{T \times 10^3 \times 2}{e}$$

where: T = Target thickness in kev

e = Molecular stopping power for protons in D_2O ice in 10^{-15} ev-cm^2

is obtained from Table II of the above paper.

Using the example cited previously for a target of 74 kev thickness we have: -

For E_p of approximately 400 kev $\quad \epsilon = 13.9 \times 10^{-15}$ ev-cm²

$$n_D \text{ atoms /cm}^2 = \frac{74 \times 10^3 \times 2}{13.9 \times 10^{-15}}$$

$$= 1.06 \times 10^{19} \text{ atoms /cm}^2$$

Thus for a D_2O ice target of 74 kev thickness one has 1.06×10^{19} atoms /cm².

Target thicknesses for the absolute cross section measurements to be discussed in Chapter IV were calculated in this manner.

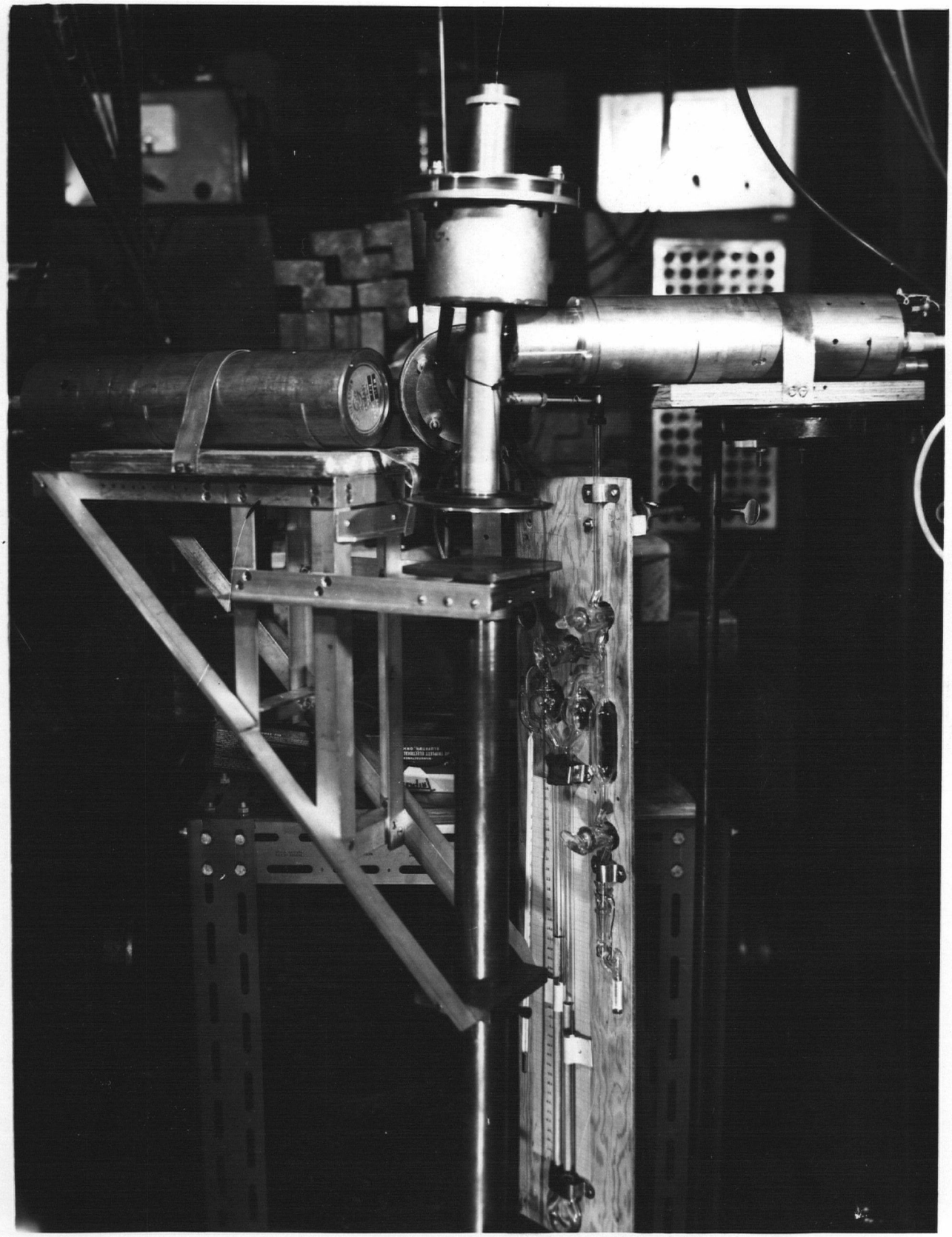

PLATE I. THE $D(p,\gamma)He^3$ APPARATUS

CHAPTER IV

THE $D(p,\gamma)He^3$ REACTION

1. INTRODUCTION

After the determination of the crystal efficiency (Ch. II) and the target thickness (Ch. III) it was possible to determine the absolute cross section and angular distribution for the $D(p,\gamma)He^3$ reaction as described below.

2. THE ANGULAR DISTRIBUTION OF $D(p,\gamma)He^3$ GAMMA RAYS

(a) Apparatus

The target chamber used for the measurements and the preparation of the D_2O targets are described in Chapter III above. The gamma counter whose efficiency was measured in Ch. II, hereafter called the "large" counter, was used to measure the intensity of the gamma radiation at the different angles.

A monitor counter, hereafter called the "small" counter, was used during the angular distribution runs. This counter is described in Appendix 1.

The large counter was fastened to an aluminum frame which could be rotated in a horizontal plane around the target chamber as shown in Plate I. The counter was set so that the crystal center was at the same height as the proton beam spot on the target, the counter was horizontal and swung in a horizontal plane with the crystal always set the same distance from the target. The small counter was held by an adjustable X-ray stand as close

to the target as possible and at an angle of approximately 90^{o} to the beam as seen in Plate I.

The low gamma yield at 0^{o}, especially at a proton energy of 300 kev, made it essential that the background during the experiments be kept at a minimum. A moveable rack holding a six inch thick lead brick layer approximately eighteen inches square was rolled over the gamma counter at 0^{o} to cut down the time dependent background. Since contaminants, especially fluorine with its 6 Mev gamma rays, in the target chamber would have added to the background the copper target plate and the end of the inner chamber were electroplated with gold using Caro-Perfection Gold Solution. The gold layer lowered the background radiation observed from the copper and brass.

(b) Electronics

The gamma ray pulses from the large counter were put onto the thirty channel kicksorter as described in Chapter II. An Isotopes Developements Limited E.H.T. Unit Type 532 supplied the high voltage for both the large counter (1000 volts) and the small counter (960 volts).

The monitor counter had a delay line pulse shaping head amplifier described by Phillips (1957). Pulses from the head amplifier were fed through a Dynatron 1049B Amplifier into two decade scalers whose discrimination levels were set such that the "lower" scaler counted from just below the gamma-ray peaks and the "upper" counted from just above the peaks so that the $D(p,\gamma)He^{3}$ gamma - ray yield was proportional to the difference in the readings of the two scalers. All discrimination levels were set and

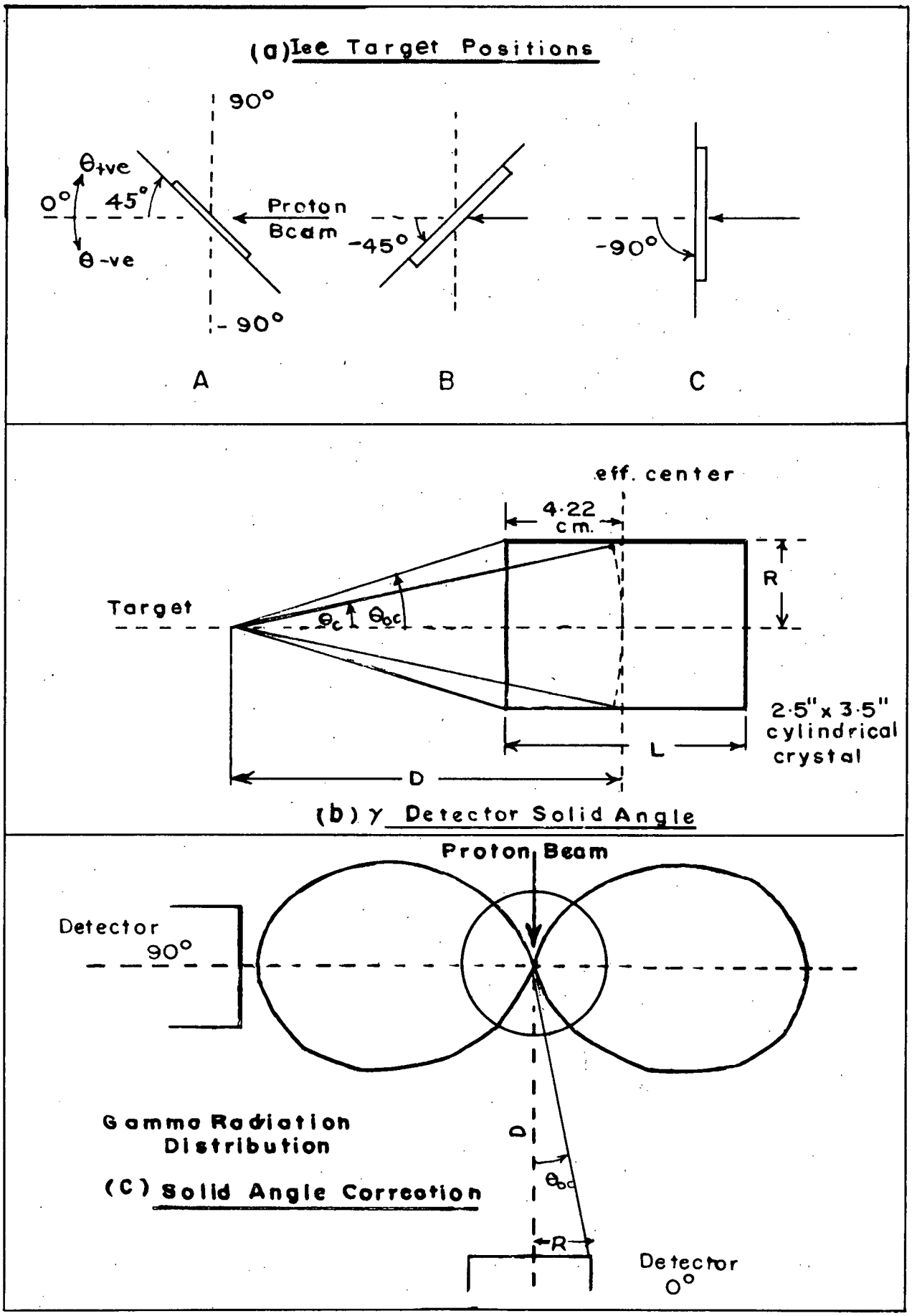
(a) Iee Target Positions
90°
θ+ve
0°
45°
θ -ve
Proton
Beam
-45°
-90°
A
B
C
eff. center
4·22
cm.
R
Target
θc
θbc
2·5" x 3·5"
cylindrical
crystal
L
D
(b) γ Detector Solid Angle
Proton Beam
Detector
90°
Gamma Radiation
Distribution
(C) Solid Angle Correction
D
θbc
R
Detector
0°

Fig. 11

linearity of the electronics was checked using the accurate mercury pulser mentioned in Chapter II.

(c) Measurements

The angular distribution of the gamma radiation was measured for proton energies of 300 kev, 600 kev and 1.0 Mev. At 600 kev measurements were made with the gamma counter at 0^{o} and 90^{o} only, while at 300 kev and 1.0 Mev measurements were also made at $\pm$ 45^{o} and 135^{o}, angles being measured as shown in Fig. 11 (a). During the various runs the target was set at position A and B so that corrections could be applied for any asymmetry due to target absorption. The yield was corrected for target absorption; the correction was 6% for gamma rays passing through the target at 45^{o}.

The lead shielding described above was used for the 0^{o} runs and therefore separate time dependent background measurements had to be taken at 0^{o} and 90^{o} as well as separate beam dependent background measurements.

The D_2O targets ranged in thickness from 75 kev to about 200 kev thick for 340 kev incident protons.

The proton beam was clipped by the molybdenum stops in the beam tube so that position fluctuations in the beam would not cause it to move over the target. The beam was defocussed so that no "hot spots" occurred on the target which would have caused deterioration. Target deterioration was checked by comparing the ratio of the counts in the monitor to the integrated beam current for successive runs and since the target deteriorated rapidly at 300 kev, the yield dropping by two-thirds after one hour of

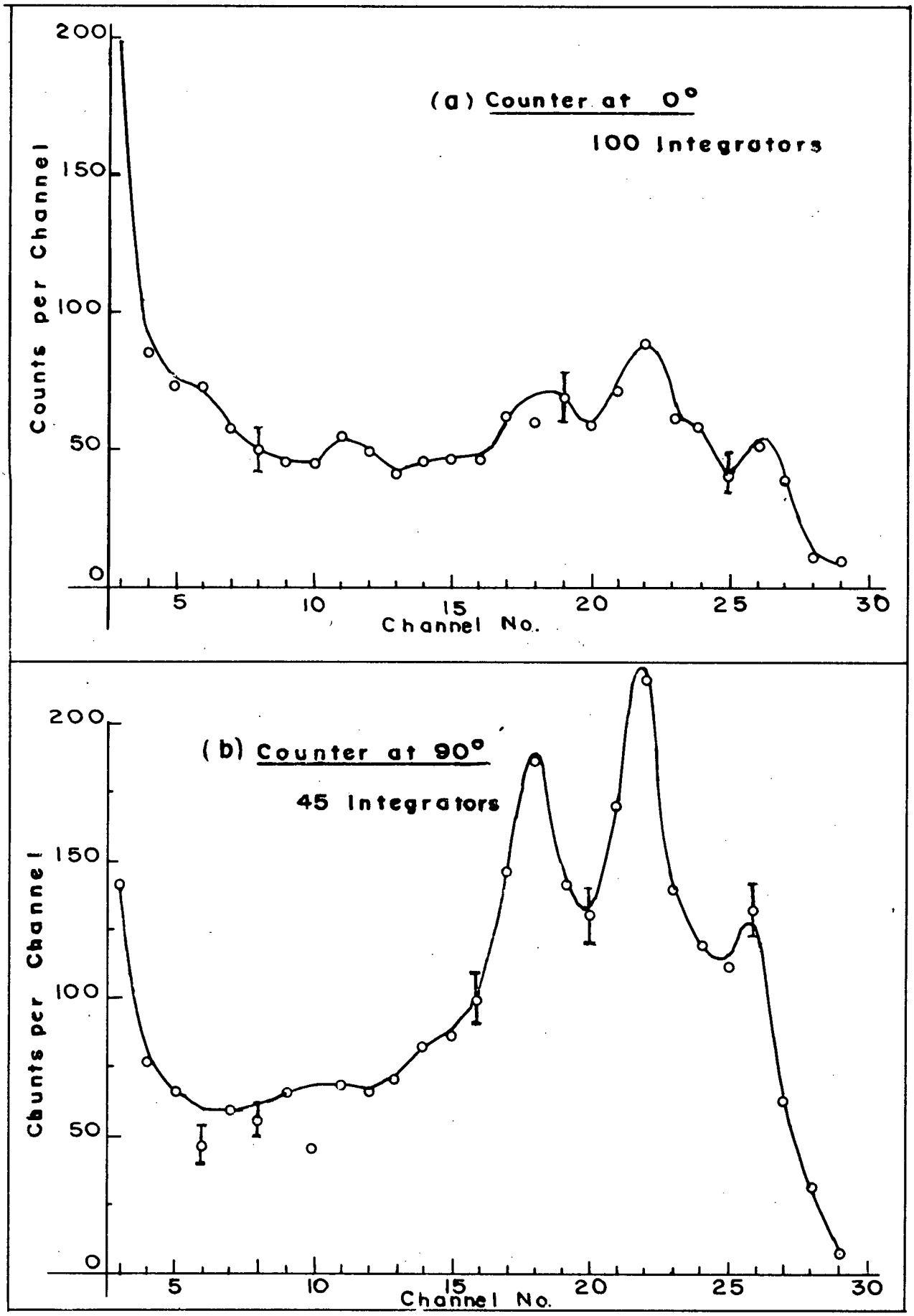

Fig. 12 $D(p,\gamma)He^3$ Spectra, Ep = 300 kev.

running of a 100 kev thick target; the targets were changed whenever appreciable deterioration was noted. At 1.0 Mev, however, the protons lose less energy in the target and targets up to 120 kev thick for 340 kev protons showed no noticeable deterioration after three hours of running time. Proton currents of about five microamperes were used on all the angular distribution runs.

An experimental check was made on the solid angle effect at 1.0 Mev by doing angular distribution measurements for a distance of 15.82 cm from the target (10.01 cm. from the counter face to the outside of the target chamber), 22.37 cm. from the target (16.56 cm. from the counter face to outside target chamber). Comparison of the results at the two different distances were used to check solid angle corrections computed from the geometry as discussed below.

A correction was made for the neutron effect from D+D reactions caused by deutrons elastically scattered by the incident protons during the $D(p,\gamma)He^3$ reaction. The number of neutrons produced at 0° by protons bombarding the heavy ice target, $N_n^p(0^\circ)$, was measured by a gamma ray insensitive neutron counter described by Ssu (1955). During the same run the number of gamma-ray counts in the large counter was obtained at 90°, $N^p(90^\circ)$. From the observed angular distributions the number of gamma ray counts at 0° from the p+D reaction, $N_\gamma^p(0^\circ)$, could be inferred. Now the gamma ray count at 0° was due to the true counts from the p+D reaction, $N_\gamma^{p(p+D)}(0^\circ)$, plus the counts due to neutrons, $N_\gamma^{p(D+D)}(0^\circ)$. In order to determine the number of counts in the gamma - ray counter due to neutrons the sensitivity of the gamma ray counter to neutrons was measured by placing both the neutron and gamma ray counters at 0° and bombarding the heavy ice target with 1.0 Mev

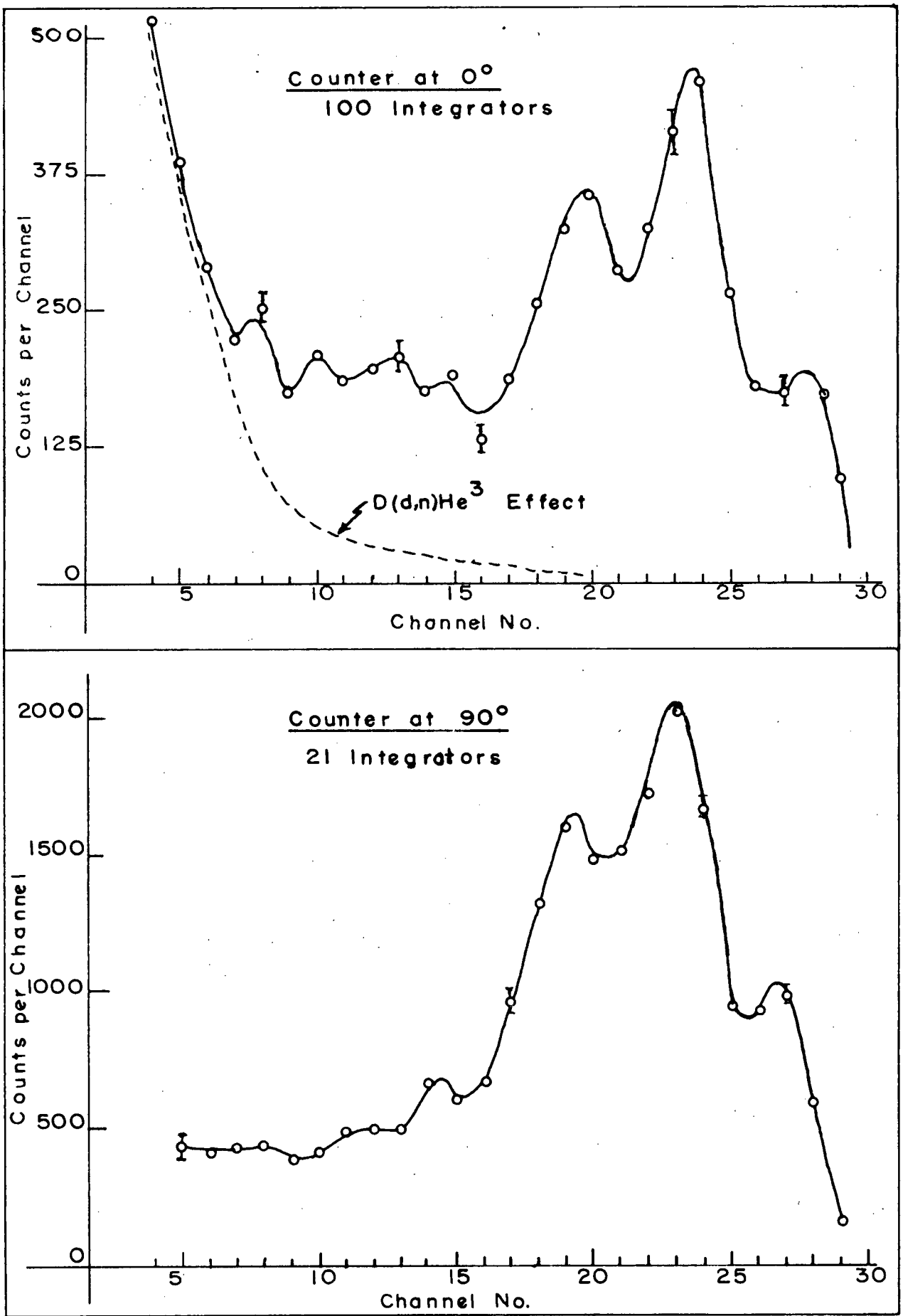

Fig.13 $D(p,\gamma)He^3$ Spectra E_p = 1·0 Mev

deuterons. Thus the number of counts in the neutron counter, $N_n^D(0^\circ)$, and the number of counts in the gamma ray counter, $N_\gamma^D(0^\circ)$ were obtained. Since no capture gamma rays are produced directly by the $D(d,n)He^3$ reaction the ratio of these two counts determines the relative efficiencies of the two counters for neutrons alone. Therefore: -

$$N_\gamma^{P(D+D)}(0^\circ) = N_n^P(0^\circ) \times \frac{N_\gamma^D(0^\circ)}{N_n^D(0^\circ)}$$

This number of counts observed in the gamma ray counter must be subtracted from the number of counts observed in the gamma counter from the $D(p,\gamma)He^3$ reaction.

The efficiency of the neutron counter is dependent on the energy of the neutrons and the average energy of the neutrons due to the secondary reaction when protons bombard the target is likely to be less than the energy of the $D(dn)He^3$ neutrons at 0°. The relative efficiencies of the neutron counter and gamma ray counter were also measured using the lower energy neutrons produced by the $D(dn)He^3$ reaction at 90°. In the calculations given below the average value for the efficiency obtained at 0° and 90° was used in making this correction.

The effect of the neutrons at 0° could also be seen by the distortion produced in the lower portion of the gamma ray spectrum at 0° when compared to the gamma ray spectrum at 90° where the neutron effect was very small as shown in Fig. 13. Since the shape of the distortion to the zero degree curve has much the same shape as the spectrum produced in this counter ~~produced~~ by neutrons it has been assumed that this distortion is produced

by the secondary neutrons. Therefore a correction for this neutron effect can be made by subtracting a sufficient number of counts from the zero degree spectrum to give it the same shape as the 90° spectrum. Reasonable agreement was obtained for these two different methods of making the neutron correction. The effect of the neutrons at 1.0 Mev. appears to have been somewhat greater than that used by Griffiths and Warren (1955) at the same energy, possibly because the latter authors compared curves taken at 0° and 45°. If at 45° there was some neutron distortion of the curve then the correction they applied would have been too small.

(d) Results

Since the gain of the system and the position of the spectrum on the kicksorter was not the same for all runs the number of counts for each run was obtained by summing the number of counts in the kicksorter channels corresponding to a definite energy range. For 1.0 Mev this energy range was chosen as 4.5 to 6.5 Mev which included the main peaks due to the $D(p,\gamma)He^3$ gamma rays and excluded as much of the low energy spectrum as possible, since this portion was distorted by background and neutron effects.

The energy region over which the kicksorter counts were summed was chosen slightly higher at 0° than at 90° by an amount necessary to correct for the Doppler shift in the emitted gamma rays (Griffiths & Warren, 1955).

A typical calculation is shown below: -

Table II

Calculation of the $D(p,\gamma)He^3$ Angular Distribution

E_p = 1.0 Mev. Target at + 45°

	$\theta = 0^\circ$	$\theta = 90^\circ$
Time	13.9 min.	3.3 min.
Beam	50 integrators	10 integrators
No. of counts in peak	2679	7941
Time background	150	36
Beam background	677	99
Neutron effect correction	122	--
Total correction	949	135
D (p, γ) yield	1730	7806
Absorption correction	1730/.94 = 1842	--
Monitor uncorrected	65030	12057
Time background	63	16
Beam background	948	145
Monitor corrected	64019	11896
N_γ /N monitor	Y_{0° = 0.0287	Y_{90° = 0.656

$$\text{Yield Ratio} \quad \frac{Y_{0^\circ}}{Y_{90^\circ}} = \frac{0.0287}{0.656} = 0.0437$$

The experimentally observed angular distributions consisted of a predominant component proportional to $\sin^2\theta$ plus a non zero contribution at 0° suggesting the presence of an isotropic component. If we assume that the true distribution is of the form -

$$N(\theta)d\omega = A(\sin^2\theta + b)d\omega$$

as shown in Fig. 11(c), then the experimentally observed distribution will be distorted from this form by the finite solid angle of the detector. In order to determine "b" it is necessary to correct for this distortion.

Integration of this angular distribution function over the whole sphere determines the total yield as

$$No = 4\pi A(2/3 + b)$$

which will be used in computing the yield of the reaction in section 3.

If the angular aperture of the large gamma ray counter has a half angle of θ_c subtended at the target as shown in Fig. 11(b) then at 0° the counting rate should be

$$N_c(0^\circ) = 2\pi\epsilon \times \int_0^{\theta_c} \sin\theta\, N(\theta)\, d\theta$$

$$= 2\pi\epsilon A\left[2/3 - \cos\theta_c + \frac{\cos^3\theta_c}{3} + b(1-\cos\theta_c)\right]$$

where ϵ is the crystal efficiency as defined in Ch. II.

At 90° if we assume that the gamma ray flux is constant across the

whole face of the crystal and has the value obtained from the above angular distribution function at 90°, then the observed count at 90° should be -

$$N_c(90^{\circ}) = 2\pi \in A(1+b)(1 - \cos\theta_c)$$

The ratio of the observed counts at 0° and 90° is then -

$$\frac{N_c(0)}{N_c(90)} = \frac{\dfrac{2/3 - \cos\theta_c + \dfrac{\cos^3\theta_c}{3}}{1 - \cos\theta_c} + b}{1+b}$$

$$\approx \frac{\dfrac{2/3 - \cos\theta_c + \dfrac{\cos^3\theta_c}{3}}{1 - \cos\theta_c} + b \qquad \text{----------A}$$

since $b \ll 1$ as will be seen from the results below. Thus the value of b which is of interest can be obtained from the observed ratio by subtracting from that ratio the first term above depending on the counter solid angle. This term represents the counting rate in the crystal at 0° from the $\sin^2\theta$ component due to the finite solid angle of the counter.

There was some uncertainty concerning the value of θ_c that should be used in the above expressions. The solid angle to the effective centre θ_c as shown in Fig. 11(b) is satisfactory for the isotropic component since

this produced a uniform flux across the crystal face which corresponds to the conditions used to determine the efficiency and effective centre (Ch. II). But the $\sin^2\theta$ component did not produce a uniform flux over the crystal; the flux was greatest at the outer edges so that the effective solid angle could have been between θ_c and θ_{oc} shown in Fig. 11(b). In order to check the validity of using θ_c as the solid angle, measurements of the ratio of counts at 0° to counts at 90° were taken for two different target to counter distances as described in section C. These two distances corresponded to $\theta_c = 11^\circ 20$ for $D_{10} = 15.82$ cm. and $\theta_c = 8^\circ 5$ for $D_{16} = 22.37$ cm. The ratios for the yield at 0° to the yield at 90° obtained at 1.0 Mev for the $D(p,\gamma)He^3$ reaction were

$$R_{10} = 0.0587 \qquad \text{and} \qquad R_{16} = 0.0461$$

These ratios were obtained after background and neutron effect corrections and except for solid angle effects should have been the same. Solid angle corrections were computed for the above angles using formula A above giving for the first term on the right side the value 0.0194 for the smaller distance and 0.0099 for the larger one. Thus the two values obtained for "b" are 0.0393 and 0.0362. These are in agreement to about 10%; the accuracy of the measurements was not greater than this and consequently we can conclude that the solid angle effect has been properly corrected for to this order of accuracy.

Then, using this value of the $\sin^2\theta$ distribution we can calculate the value of the isotropic component b.

For the example cited in Table II we have -

$$b = 0.0437 - 0.0194 = 0.0243$$

The other results are calculated similarly for the other trials. The means of the results are given in Table III.

Estimated Errors:

Distance	15.82 ± .2 cm =	15.82 ± 2%
Solid Angle	± 5%	
Neutron effect	± 10%	

The uncertainty in the counting statistics was calculated as follows:

Uncertainty in counts N is $\pm\sqrt{N}$

Percentage error in $\frac{N_\gamma}{N_m}$

$$= \pm\sqrt{\frac{\sqrt{N_\gamma}}{N_\gamma} + \frac{\sqrt{N_m}}{N_m}} \times \frac{N_\gamma}{N_m}$$

$$= \pm\sqrt{\frac{1}{N_\gamma} + \frac{1}{N_m}} \times \frac{N_\gamma}{N_m}$$

N_γ is the sum of total number of counts in the uncorrected gamma spectra plus the total number of time dependent counts plus the total number of beam dependent counts, the last two being considered before normalizing factors

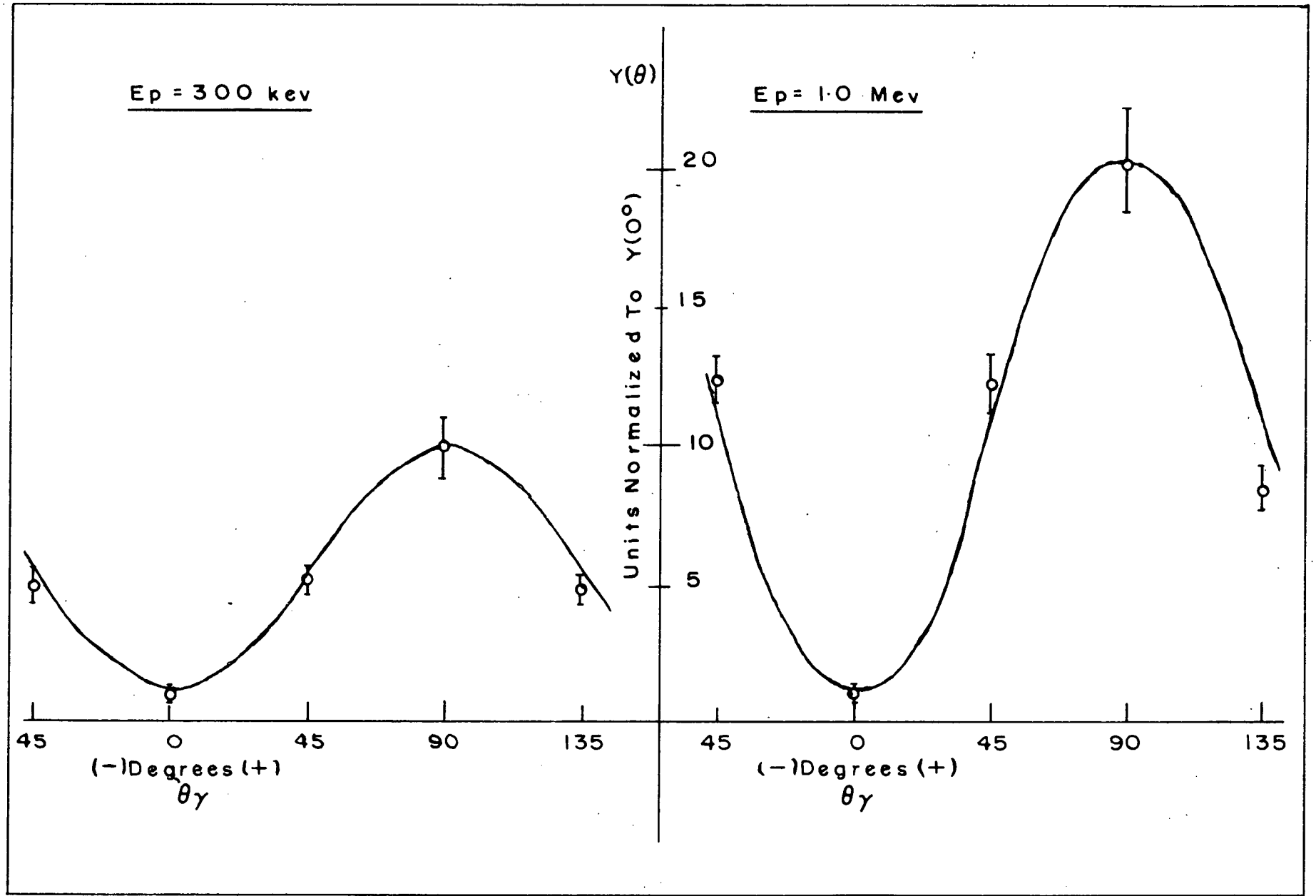

Fig. 14 Angular Distribution of Gamma Radition from $D(p,\gamma)He^3$

were used. N_m is a similar sum for the monitor counts.

The percentage error in the $\frac{N_\gamma}{N_m}$ ratio was calculated at 0° and 90° and called E_1 and E_2 respectively.

Thus the percentage error due to counting uncertainties in the final ratio is -

$$E = \pm \sqrt{E_1^2 + E_2^2}$$

This percentage error was calculated for each energy and the final estimated percentage error is

$$\Delta b = \pm \sqrt{(3)^2 + (5)^2 + (10)^2 + (E)^2}$$

The final results: -

Table III

Angular Distribution Results

E_p	Distribution	R_o/R_9
1.0 Mev	$\sin^2\theta$ + .024 ± .003	.043 ± .005
0.6	$\sin^2\theta$ + .032 ± .004	.052 ± .006
0.3	$\sin^2\theta$ + .0795 ± .010	.099 ± .013

3. ABSOLUTE CROSS SECTION MEASUREMENT OF $D(p,\gamma)He^3$

(a) Apparatus

The apparatus used for these measurements was the same as used for the angular distribution measurements except that the monitor counter was

not used and the large counter was held on a larger, heavier stand since it was shielded by about seven inches of lead above it and on the sides. The counter was set at 90° to the beam and about 13 cm. from the target so that the center counter line was horizontal with the target spot. The target plate was set at 45° to the beam, position A in Fig. 11(a). The large counter electronic system was identical to that used during the angular distribution measurements.

(b) Measurements

The absolute cross section was measured at a proton energy of 300 kev and 1.0 Mev for several D_2O targets of thicknesses from 41 kev to 76 kev for 340 kev incident protons using the D_2O dispenser calibration curve of Fig. 9. A careful check was kept on target deterioration by dividing the runs into separate trials and noting the ratio of gamma ray yield to integrated beam current. If this yield started to decrease, as it did after 40 integrators at 300 kev, the target was removed and another target made. Beam dependent and time dependent backgrounds were taken. The target spot was clipped by the stops in the beam tube of the target chamber and the beam was defocussed so that the beam formed a uniform spot on the target. The beam could be seen very easily as a bright blue glow on the ice target. A low current of about one microampere was used so that target deterioration from the heating effect of the beam was reduced.

(c) Calculations

The absolute cross section was calculated for each target thickness by taking into account the number of D atoms per square centimeter using the

figures of Wenzel & Whaling (1952), the number of protons from the known calibration of the current integrator, and the solid angle and efficiency of the counter.

Cross Section

If $$\sigma(\theta) = A(\sin^2\theta + b)d\omega$$

where A has the dimensions square centimeters per unit solid angle when integrated over all angles this gives the total cross section in square centimeters.

$$\sigma_T = 4\pi A\,(2/3 + b)$$

Then A can be related to the observed count at 90° as follows: -

$$N_c^{(90^\circ)} = \epsilon N_p N_D \omega_\gamma A(1+b)$$

Then: -

$$\sigma_T = \frac{4\pi N_c^{(90^\circ)}}{\epsilon N_p N_D \omega_\gamma} \times \left(\frac{2/3+b}{1+b}\right)$$

where: - N_p = No. of incident protons

N_D = No. of D atoms / cm^2

ϵ = efficiency of counter = .61

ω_γ = solid angle of counter

Efficiency of counter 0.61 for 6.14 Mev gamma rays: -

Solid angle, $$\omega_\gamma = \frac{\text{Area of crystal}}{(\text{Distance from eff. center to target})^2} = \frac{31.67}{(15.82 \pm .2)^2}$$

$$N_P = \frac{I \times 106}{1.602 \times 10^{-13}} \qquad N_D = \frac{2T \times 10^3}{e \times \cos 45^\circ}$$

where I = Beam current in integrators
(106 microcoulombs per integrator)

T = Thickness of targets in kev from Fig. 9.

e = Molecular Stopping power for protons in D_2O ice in 10^{-15} ev - cm^2

Collecting all the constants in the cross section expression we have: -

$$\sigma_T = \frac{N_c(90)^e}{IT} \times \frac{2/3 \quad b}{1 \quad b} \quad (.871 \times 10^{-31}) \ cm^2$$

From Table III, we have the values

At E_p = 300 kev, b = 0.0795

E_p = 1.0 Mev, b = 0.0239

A typical calculation follows:

Table IV

Typical Cross Section Calculation

E_p = 300 kev 15 integrators	63 kev thick target 17.3 minutes
No. of Gamma Rays above $E_{\frac{1}{2}}$	1155
Time dependent background	176
Beam dependent background	25
No. of Gammas (corrected)	954
Corr. for absorption in 1/16 inch brass	$\frac{954}{.94} = 1015$
Target thickness	63 kev
Molecular stopping power	13.8×10^{-15} ev-cm

Substituting values, we have -

$$\sigma_T = \frac{954 \times 13.8}{15 \times 63} \times \frac{0.6667 + 0.0795}{1 + 0.0795} \times .871 \times 10^{-31} \text{ cm}^2$$

$$\sigma_T = 0.891 \times 10^{-30} \text{ cm}^2$$

Estimated Errors: -

Counter to target distance	15.82 ± 0.2 cm $= 15.82 \pm 1.2\%$
Counting statistics	$\pm\sqrt{N_\gamma + T + B}$
Molecular Stopping Power	$\pm 4\%$
Current Measurements	$\pm 2\%$
Counter Efficiency	$\pm 2\%$
Target thickness	$\pm 10\%$

Thus the percentage uncertainty in the total cross section is the square root of the sum of the squares of the above percentage uncertainties and is eleven per cent for both the 300 kev and 1.0 Mev runs (ignoring the less than one percent error due to the uncertainty in b). The estimated error of the target thickness was obtained by noting the consistency between the cross section values for the different runs. These values varied by ten percent so this was taken as an estimate of the uncertainty in the thickness of the D_2O targets.

The measured values of the absolute cross section of the $D(p,\gamma)He^3$ reaction are

$(0.898 \pm 0.097) \times 10^{-30}$ sq. centimeters at $E_p \doteq 300$ kev

and $(3.24 \pm 0.35) \times 10^{-30}$ sq. centimeters at 1.0 Mev

These values are slightly smaller than those quoted by Griffiths and Warren (1955) and Fowler (1949) but are within the $\pm 50\%$ error stated by these authors. The estimated error for the present results is about five times less than that quoted by the above workers.

APPENDIX

Efficiency Measurement of a 1.75 inch X 2 inch NaI Crystal

The efficiency of the monitor counter used in the angular distribution measurements of Chapter IV has been measured for the 6.14 Mev gamma rays from the 340 kev resonance of F^{19} $(p,\alpha,\gamma)O^{16}$. This counter had a 1.75 inch diameter by 2 inch long Harshaw sodium iodide thallium activated scintillation crystal mounted on a RCA No. 6342 two inch photomultiplier tube inside a brass cylinder three inches in diameter and ten inches long. Dow Corning No. 200 Silicone oil with a viscosity of 10^6 centistokes at 25° C held by a sleeve cut from a toy balloon was used to ensure good optical coupling between the crystal and the phototube. The counter is shown in Plate I.

The efficiency of the counter was measured using the same equipment and procedure described in Chapter II. Measurements were made at three target to counter distances. The effective center of the crystal was determined from the inverse square plot.

The efficiency at each of the distances was calculated in the same manner as for the large crystal.

The results are given in Table IV.

The effective center was found to be 2.18 $\pm$ .71 cm. from the front of the crystal.

Table V

Efficiency of Small NaI Crystal

D + 2.18 ± .71 cm	Efficiency
43.83 ± 1.0 cm	0.379
62.98 1.0	0.402
79.68 1.0	0.384

The estimated error is about five percent giving a mean value for the efficiency of this counter for 6.14 Mev gamma rays of 0.388 ± 0.019.

Bibliography

Ajzenberg, F. and Lauritsen, T., (1955), Rev. Mod. Phys., 27, 77 - 166.

Allison, S.K., and Warshaw, S.D., (1953) Rev. Mod. Phys., 25, 779.

Chao, C.Y., (1950) Phys. Rev., 80, 1035.

Chao, C.Y., Tollestrup, A.V., Fowler, W.A., Lauritsen, C.C., (1950), Phys. Rev., 79, 108.

Crenshaw, C.M., (1942), Phys. Rev. 62, 54.

Curran, S.C., and Strothers, J., (1939), Proc. Roy. Soc., 172, 72.

Davisson, D.M., and Evans, R.D., (1952), Rev. Mod. Phys. 24, 79.

Devons, S. and Hines, M.G.N., (1949), Proc. Roy. Soc. (London), 199 A, 56.

Dosso, H.W., (1957), M.A. Thesis, University of British Columbia

Freeman, J.M., (1950), Phil. Mag. 41, 1225.

French, A.P., and Seidl, F.G.P., (1951), Phil. Mag. 42, 537.

Fowler, W.A., Lauritsen, C.C., and Tollestrup, A.V., (1949), Phys. Rev. 76, 1767.

Griffiths, G.M., and Warren, J.B., (1955), Proc. Phys. Soc. A, 68, Pt. 9, 781 - 92.

Hirschfelder, J.O., and Magee, J.L., (1948), Phys. Rev. 73, 207.

Huby, R., (1953), Progr. Nuclear Phys., 3, 177.

Lauritsen, T., (1950), Phys. Rev. 77, 617.

Phillips, G. (1957), PhD. Thesis, University of British Columbia

Robertson, L.P., (1957), M.A. Thesis, University of British Columbia

Ssu, W., (1955), M.Sc. Thesis, University of British Columbia

Tollestrup, A.W., Fowler, W.A., and Lauritsen, C.C., (1949), Phys. Rev. 76, 428.

Van Allen, J.A., and Smith, N.M., (1941), Phys. Rev. 59, 501.

Wenzel, W.A., and Whaling, W. (1952), Phys. Rev. 87, 3499.

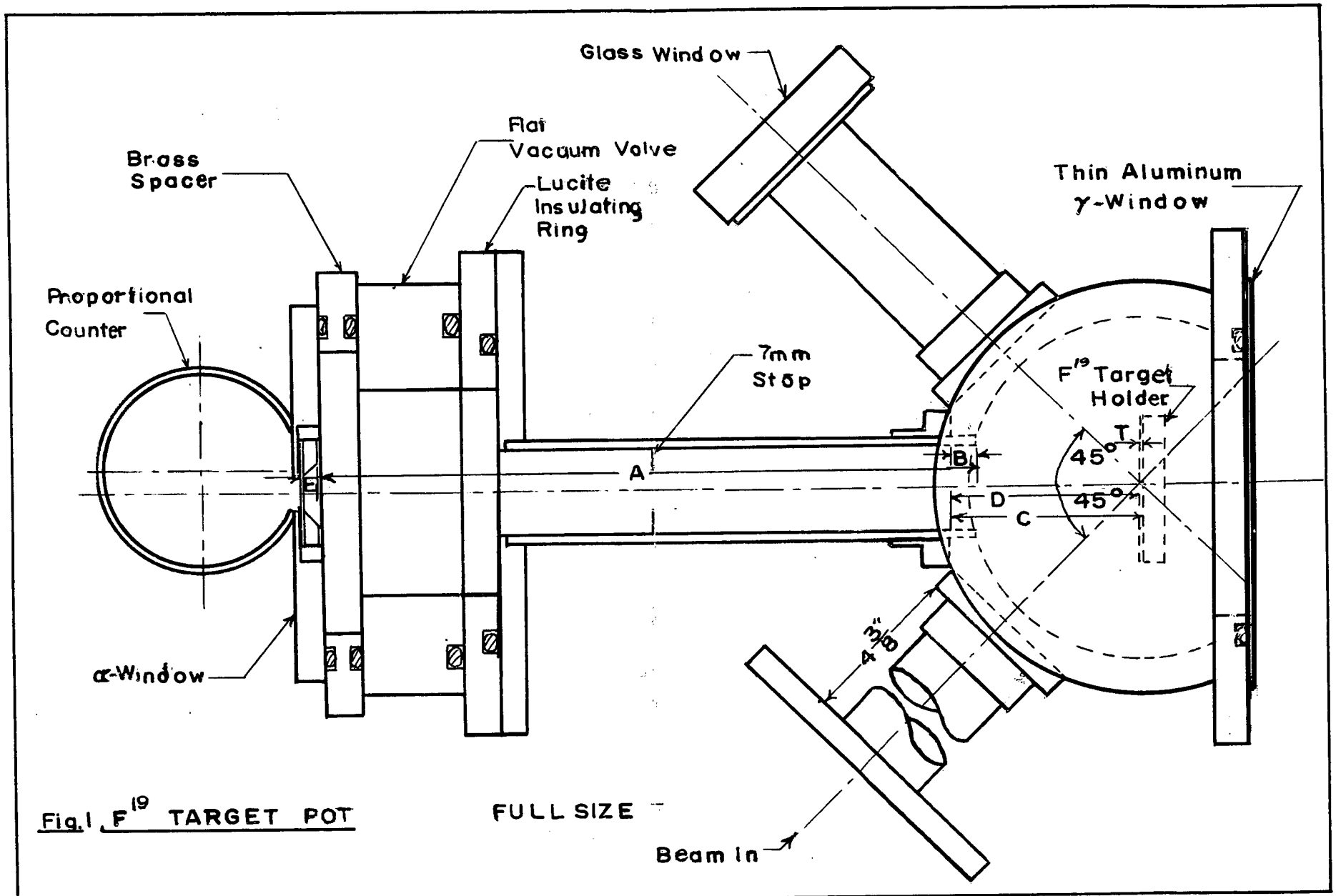

Fig. 1 F^{19} TARGET POT FULL SIZE

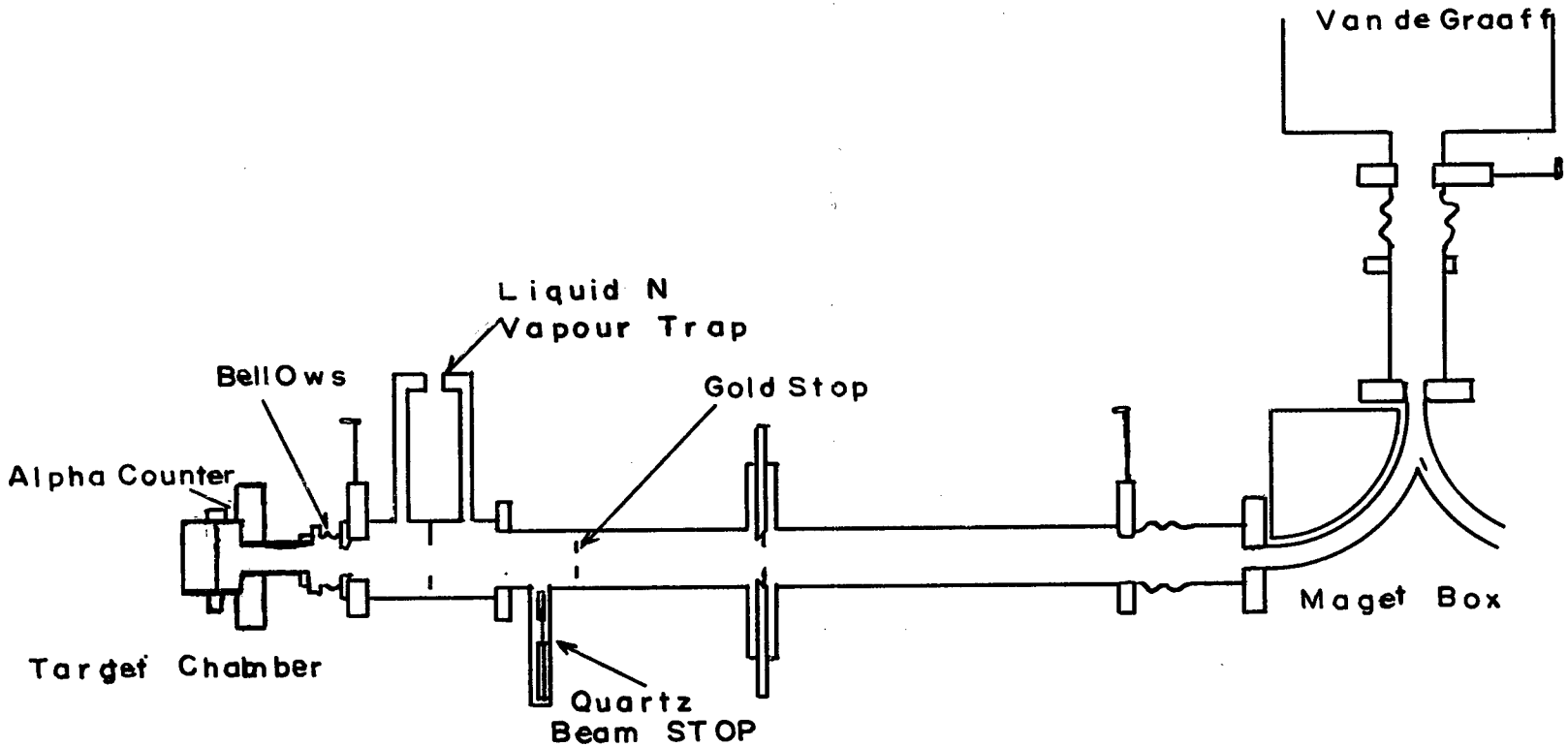

Fig. 2 Beam Tube

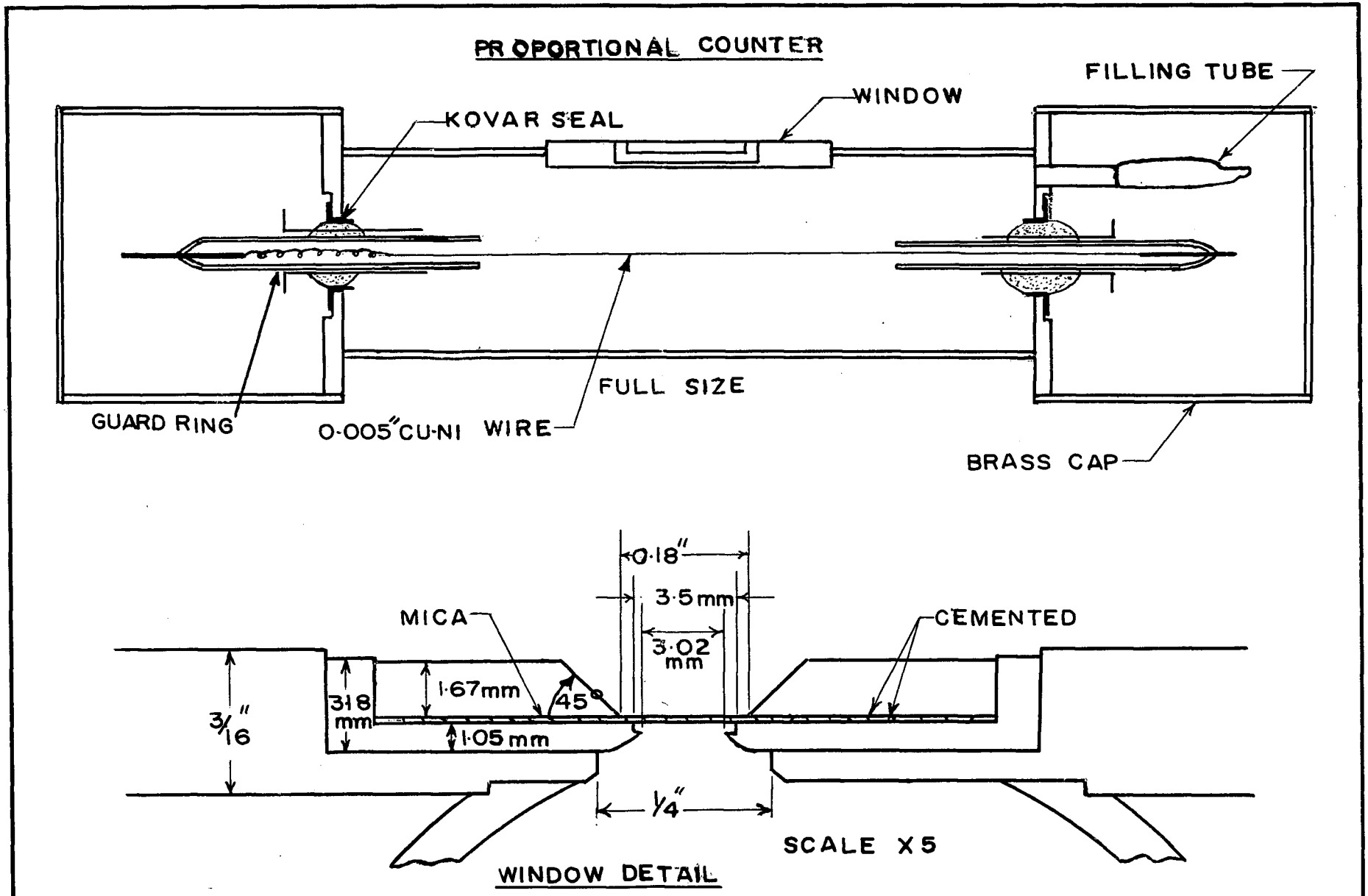

Fig. 4 Alpha Partile Counter

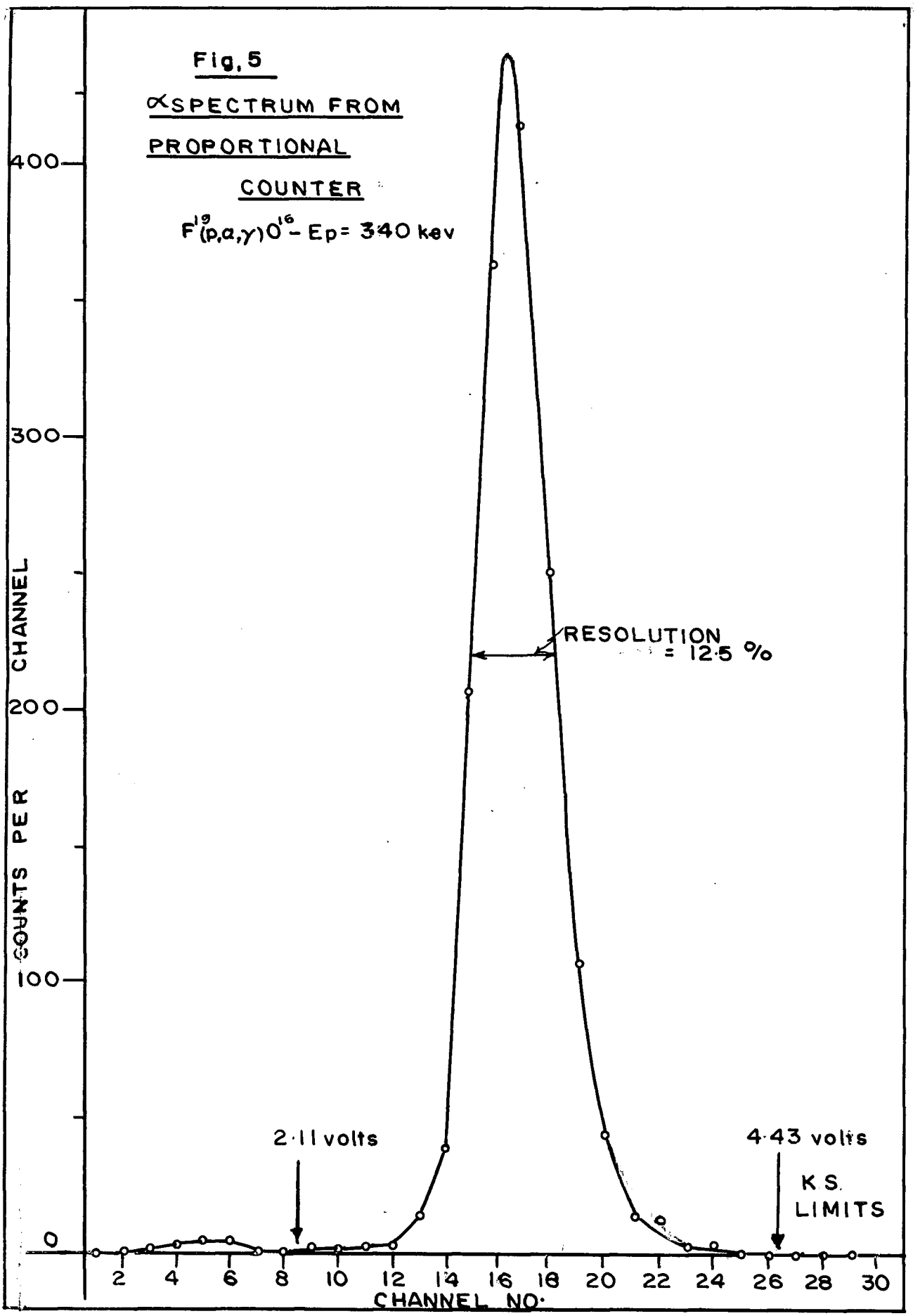
Fig, 5
α SPECTRUM FROM PROPORTIONAL COUNTER
$F^{19}(p,\alpha,\gamma)O^{16}$ - Ep = 340 kev
RESOLUTION = 12·5 %
2·11 volts
4·43 volts
K S. LIMITS
COUNTS PER CHANNEL
CHANNEL NO.
0
100
200
300
400
2
4
6
8
10
12
14
16
18
20
22
24
26
28
30

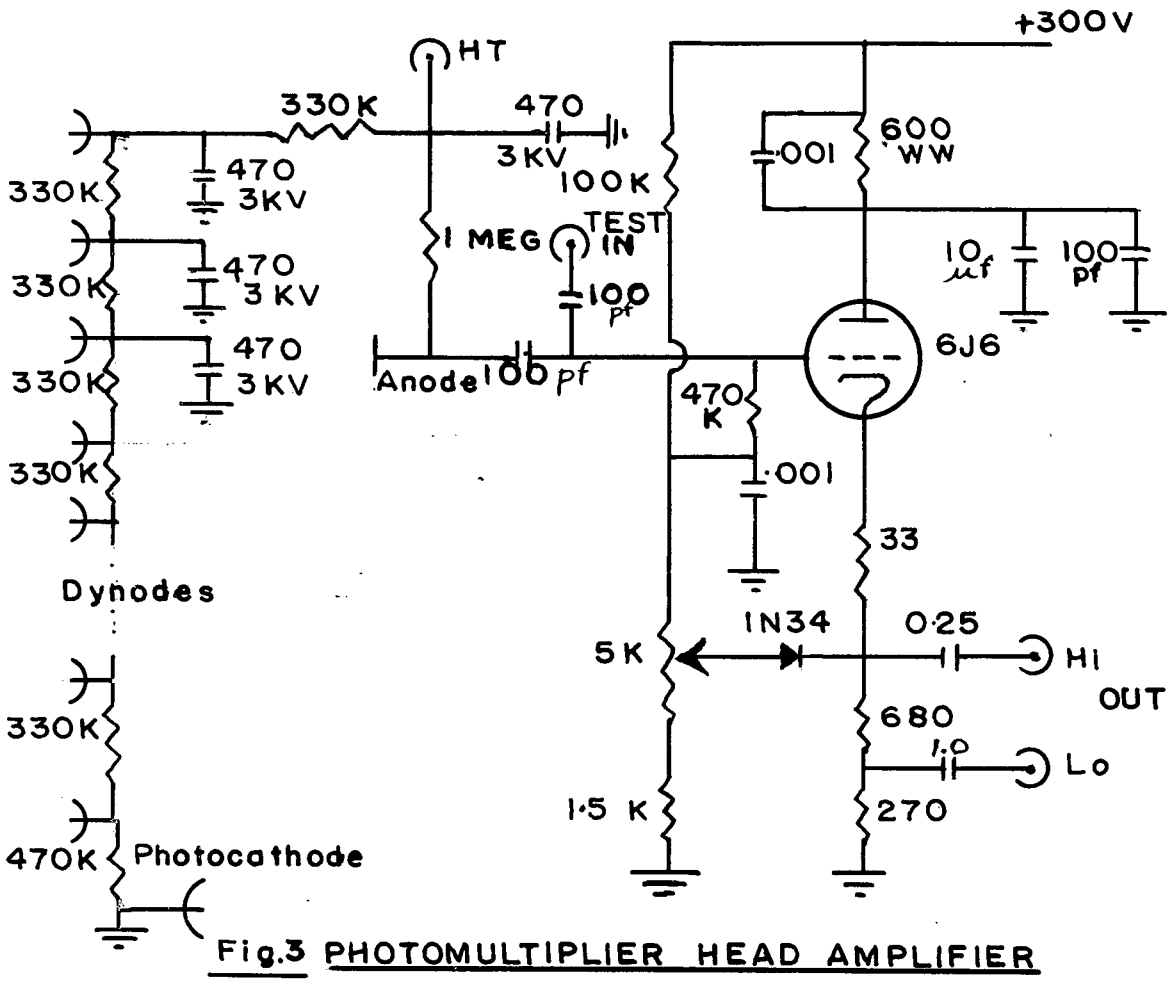

Fig.3 PHOTOMULTIPLIER HEAD AMPLIFIER

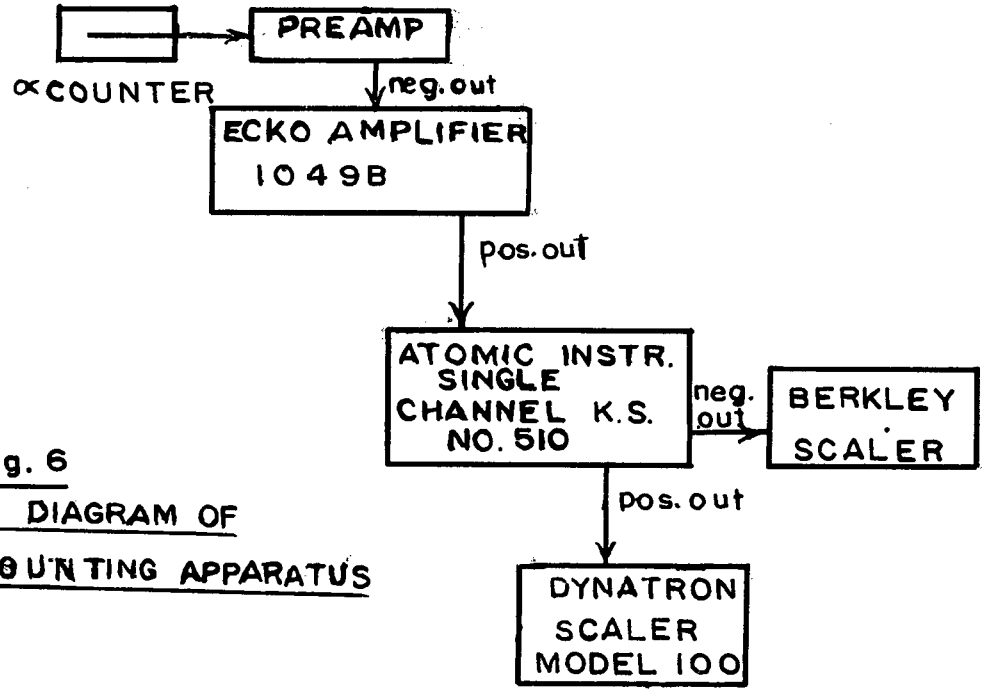

Fig. 6

BLOCK DIAGRAM OF

∝ COUNTING APPARATUS

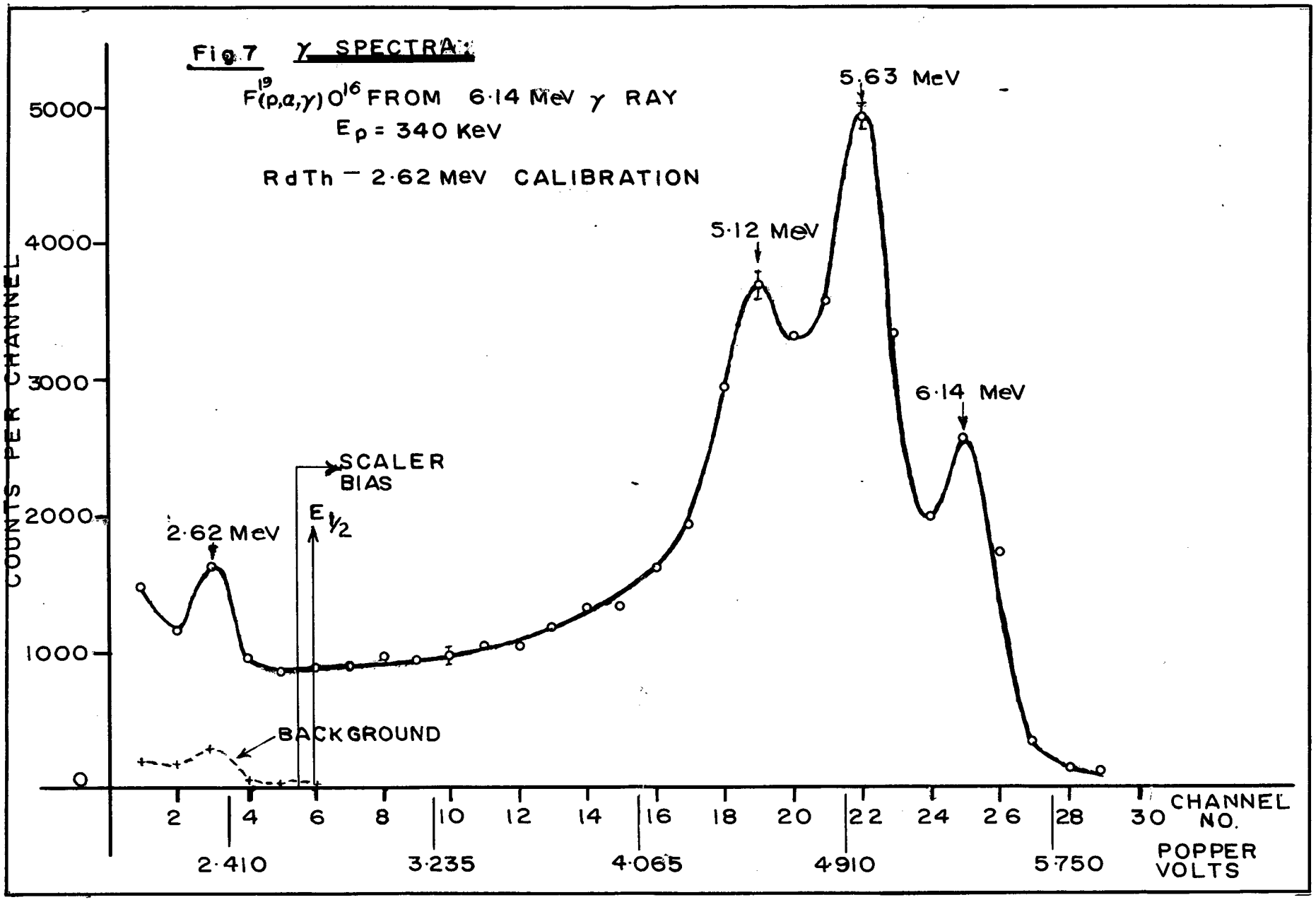
Fig.7 γ SPECTRA
$F^{19}(p,\alpha,\gamma)O^{16}$ FROM 6·14 MeV γ RAY
E_p = 340 KeV
RdTh — 2·62 MeV CALIBRATION
5·63 MeV
5·12 MeV
6·14 MeV
2·62 MeV
SCALER BIAS
$E_{1/2}$
BACKGROUND
COUNTS PER CHANNEL
5000
4000
3000
2000
1000
0
2
4
6
8
10
12
14
16
18
20
22
24
26
28
30
CHANNEL NO.
2·410
3·235
4·065
4·910
5·750
POPPER VOLTS

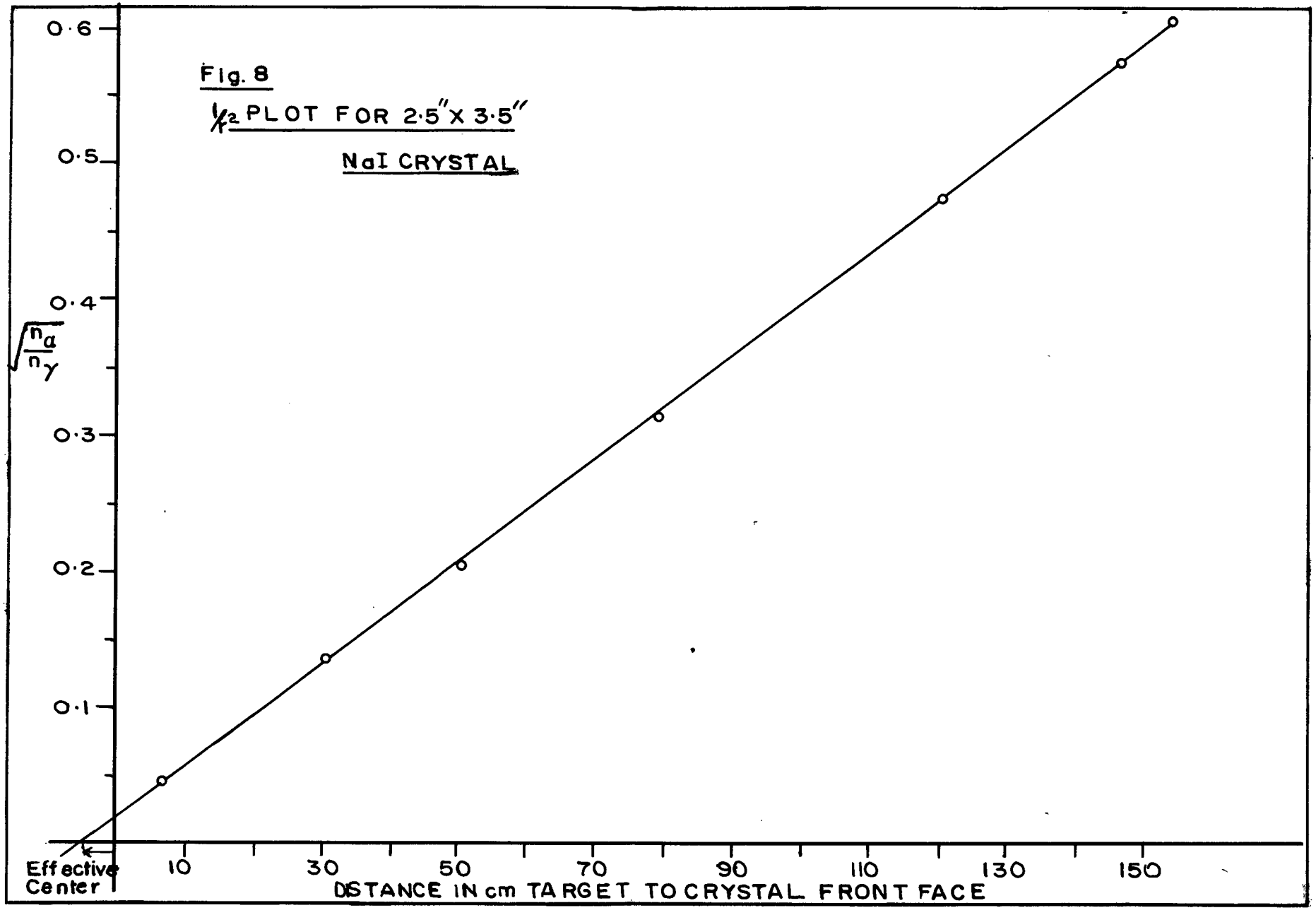
Fig. 8
1/r² PLOT FOR 2·5" X 3·5"
NaI CRYSTAL
0·6
0·5
0·4
0·3
0·2
0·1
√(n_a/n_γ)
Effective Center
10
30
50
70
90
110
130
150
DISTANCE IN cm TARGET TO CRYSTAL FRONT FACE

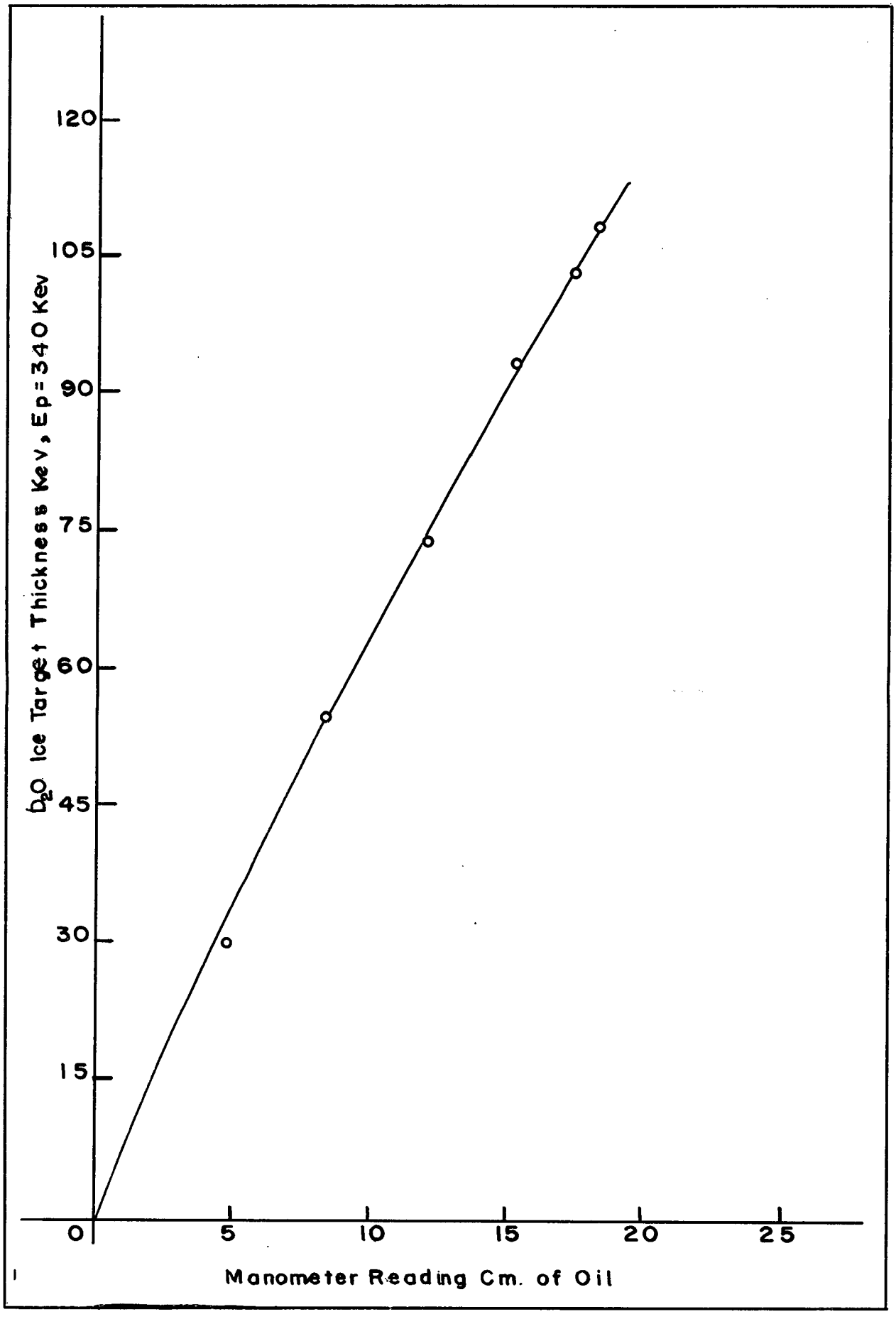

Fig. 9 D_2O Dispenser Calibration Curve

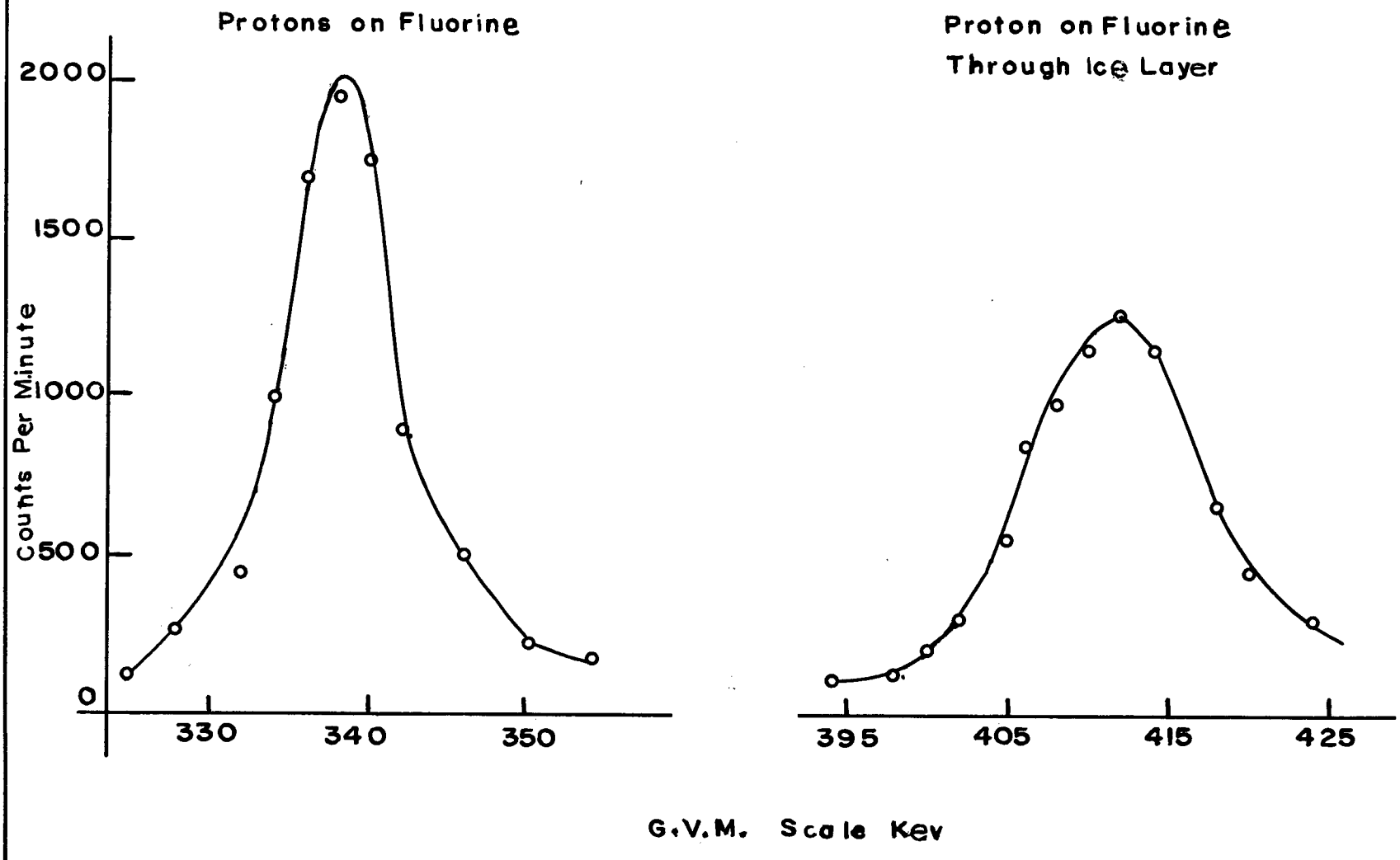

Fig. 10 D_2O Ice Target Thickness Calibration

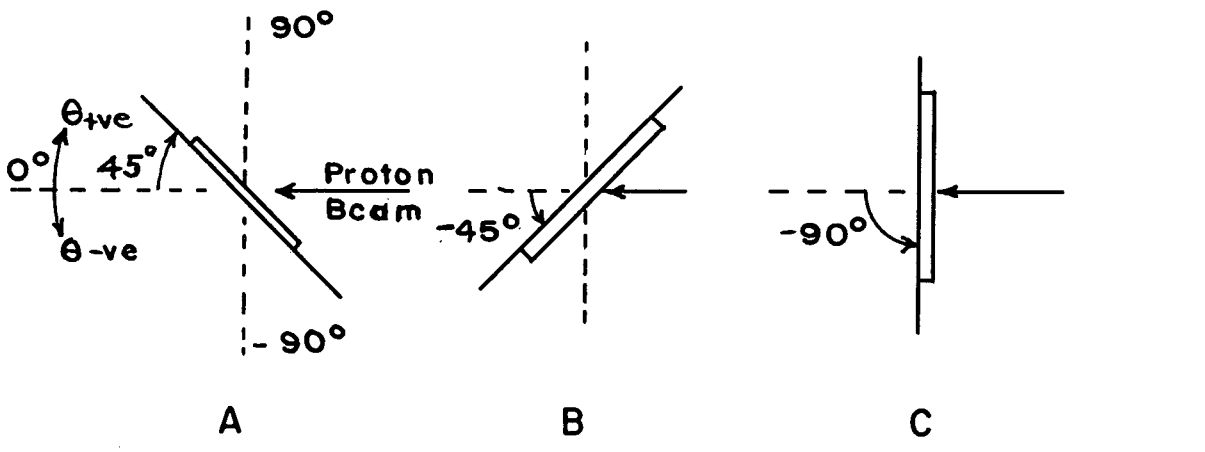
(a) Ice Target Positions
90°
θ+ve
0°
45°
Proton
Beam
θ-ve
-90°
-45°
-90°
A
B
C

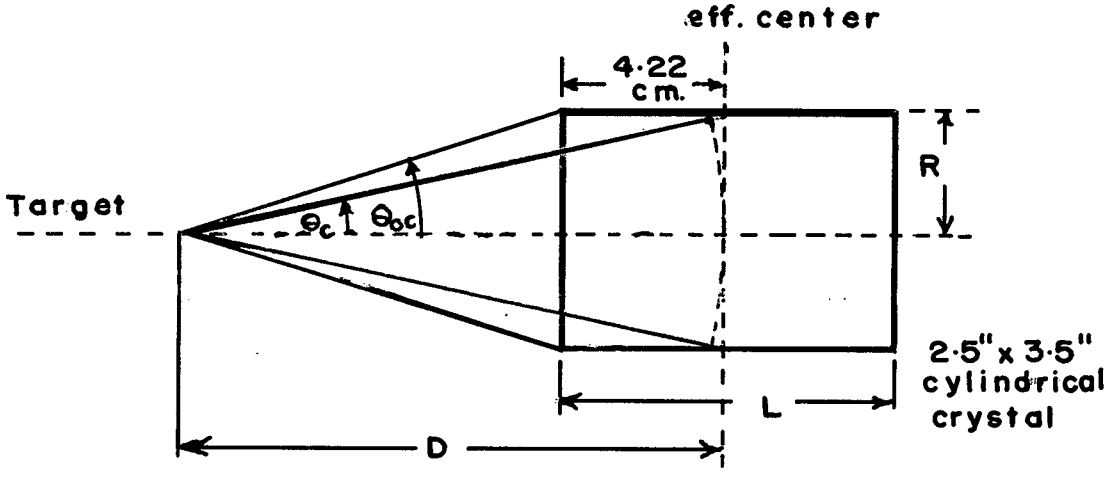
eff. center
4·22
cm.
R
Target
θc
θoc
2·5" x 3·5"
cylindrical
crystal
L
D
(b) γ Detector Solid Angle

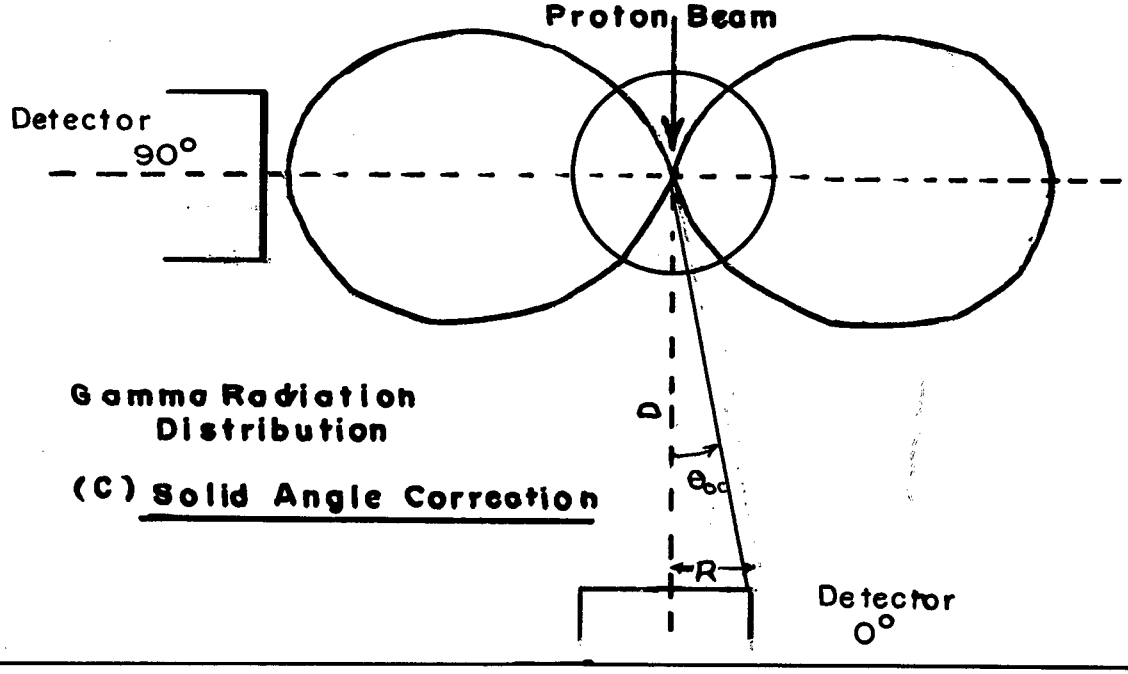
Proton Beam
Detector
90°
Gamma Radiation
Distribution
(C) Solid Angle Correction
D
θoc
R
Detector
0°

Fig. 11

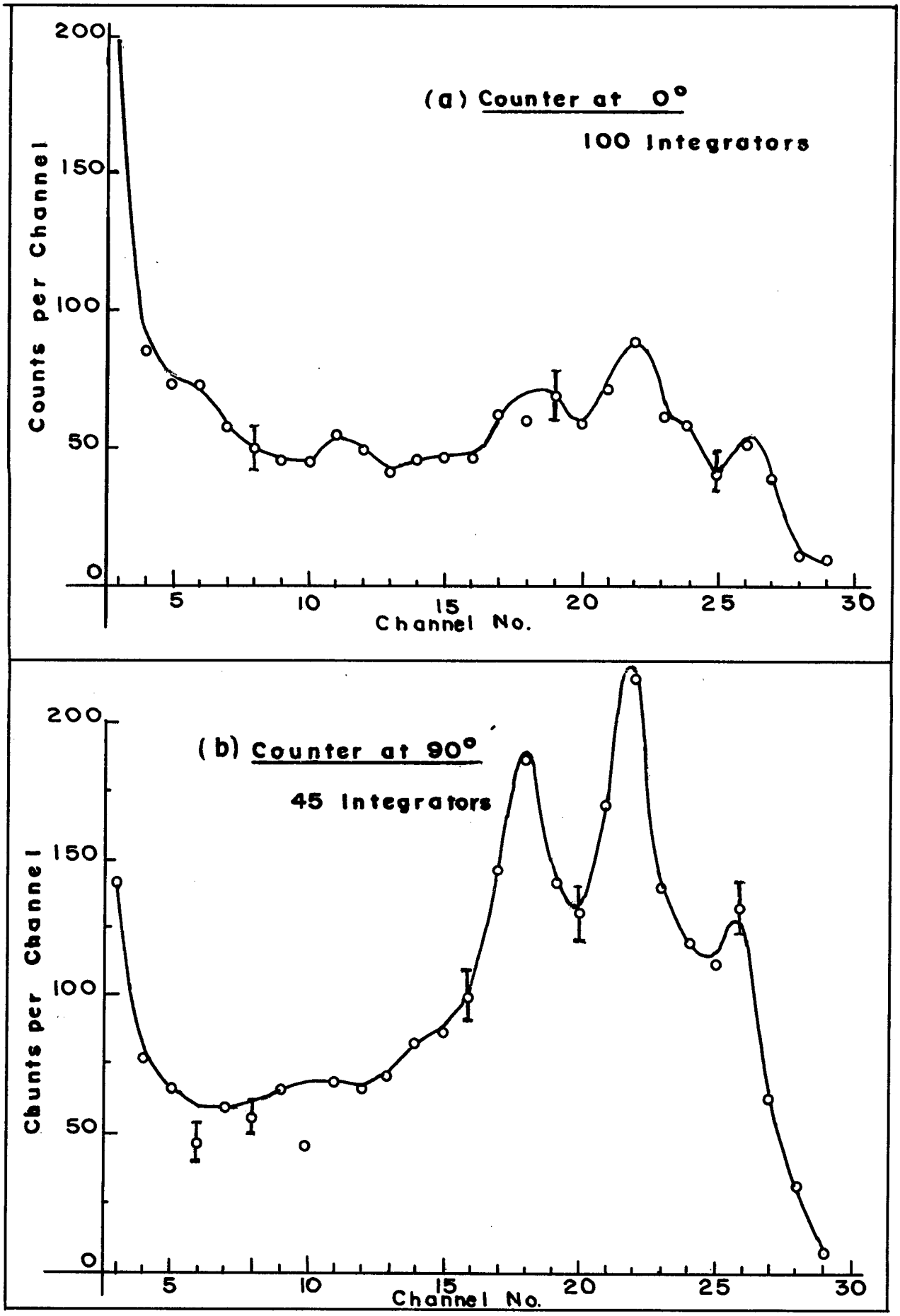

Fig. 12 $D(p,\gamma)He^3$ Spectra, Ep = 300 kev.

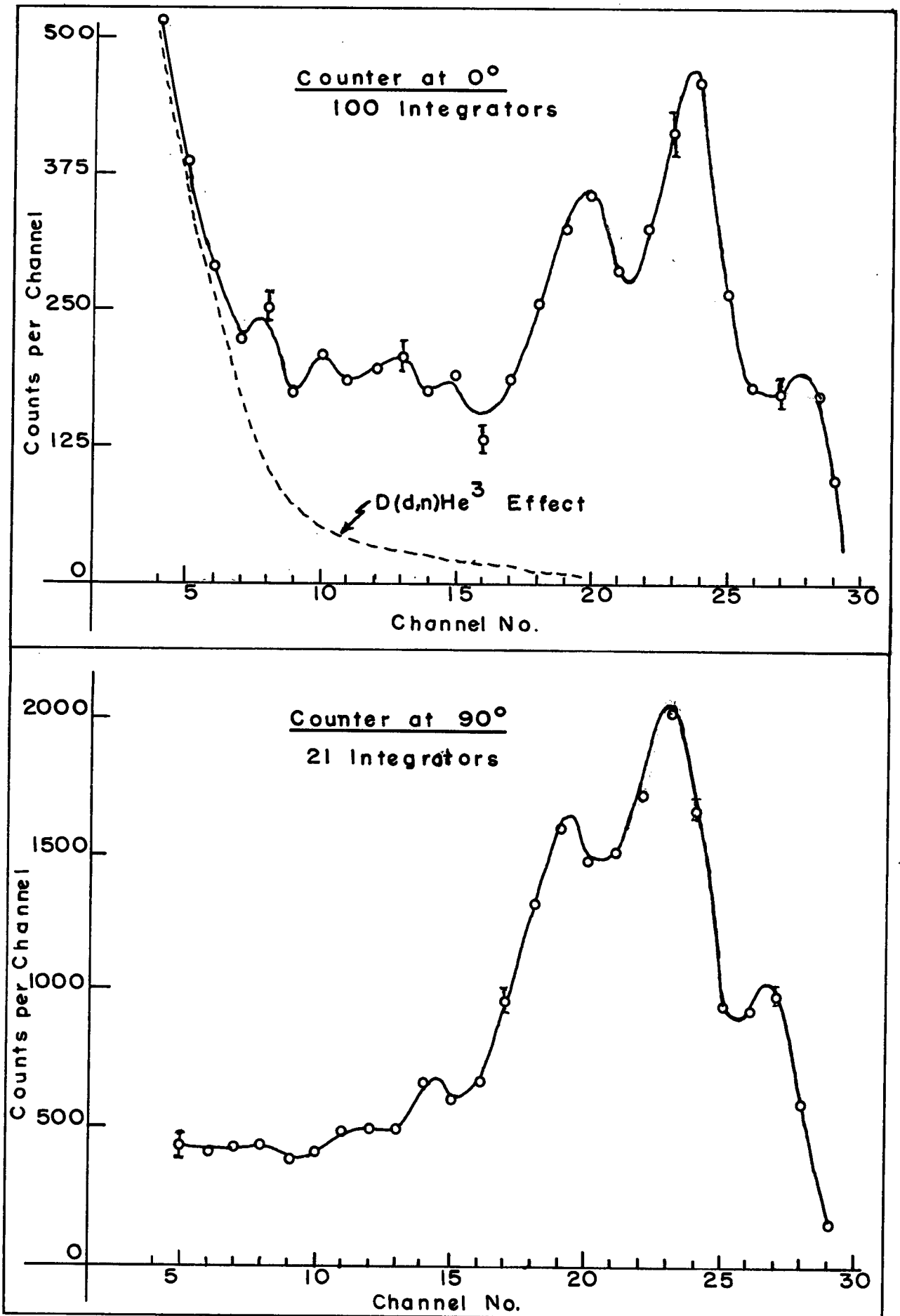

Fig.13 $D(p,\gamma)He^3$ Spectra E_p = 1·0 Mev

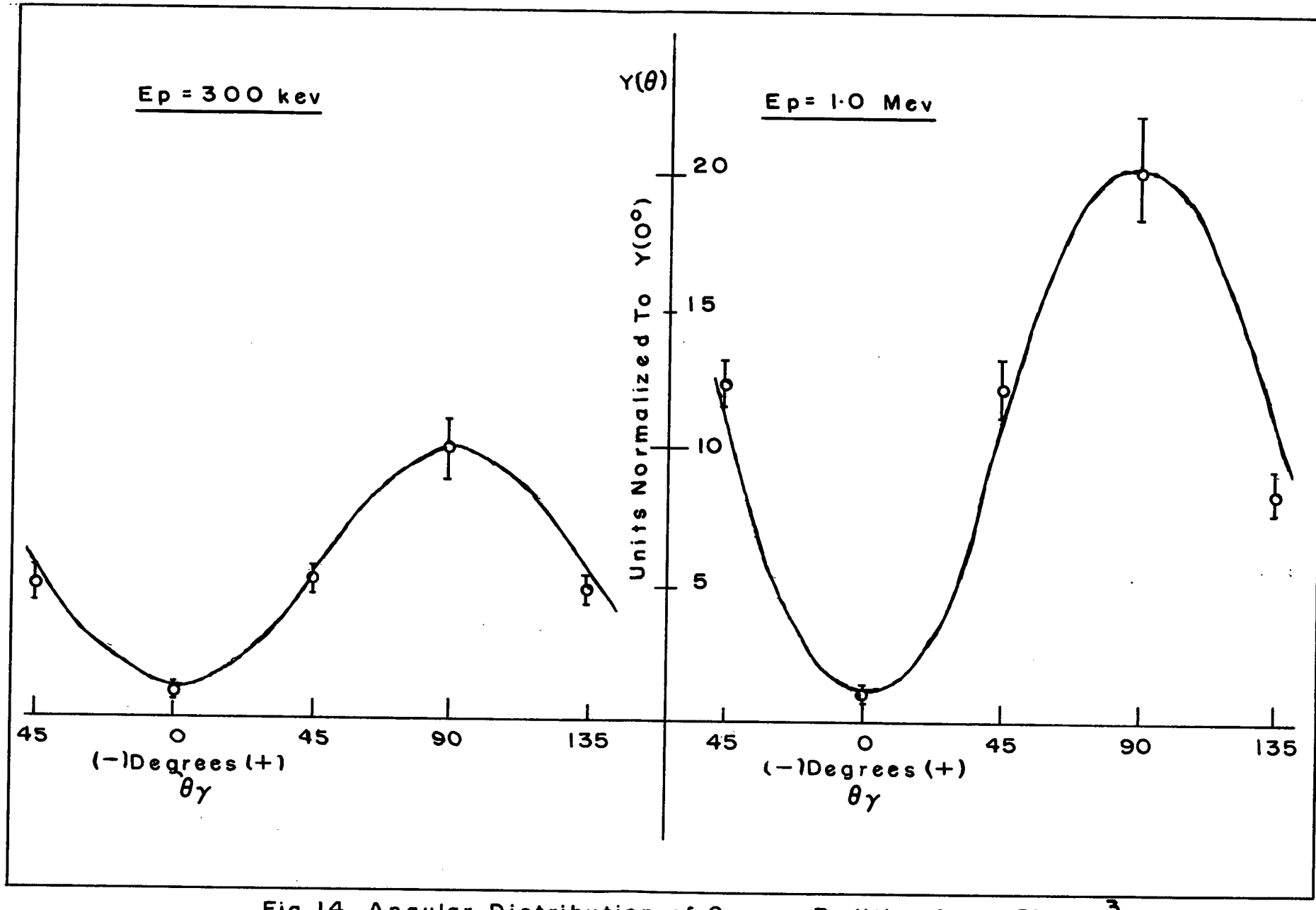

Fig. 14 Angular Distribution of Gamma Radition from $D(p,\gamma)He^3$